

# 1 Assessing models' sensitivity to the effects of forest management and 2 climate change on carbon and water fluxes in European beech forests

3

4 Vincenzo Saponaro<sup>1,2\*</sup>, Miquel De Cáceres<sup>3</sup>, Daniela Dalmonech<sup>1,4</sup>, Ettore D'Andrea<sup>4,5</sup>,  
5 Elia Vangi<sup>1</sup>, Alessio Collalti<sup>1,4</sup>

6

## 7 Affiliations:

8 1. Forest Modelling Lab., Institute for Agriculture and Forestry Systems in the  
9 Mediterranean, National Research Council of Italy (CNR-ISAFOM), Perugia, Italy;

10 2. Department for Innovation in Biological, Agri-Food and Forest Systems (DIBAF),  
11 University of Tuscia, Viterbo, Italy;

12 3. CREAM, E08193 Bellaterra (Cerdanyola del Vallès), Catalonia, Spain

13 4. National Biodiversity Future Center (NBFC), Palermo, Italy

14 5. Research Institute on Terrestrial Ecosystems, National Research Council of Italy  
15 (CNR-IRET), Porano, Italy

16 \*Corresponding author: [vincenzo.saponaro@isafom.cnr.it](mailto:vincenzo.saponaro@isafom.cnr.it)

17

## 18 Highlights

19

20 ● Modelled carbon and water fluxes under different climates and management  
21 regimes

22

23 ● Different climates increases fluxes in the north and decreases them in the south

24

25 ● 3D-CMCC-FEM and MEDFATE satisfactorily predicted productivity and latent  
26 heat

27 ● 3D-CMCC-FEM predicts carbon starvation, MEDFATE predicts stem embolism  
28 in the south

29

30 ● High thinning intensity of the stand in the south negatively affected carbon  
31 fluxes

32

### 33 **Abstract**

34 The consequences of climate change continue to threaten European forests,  
35 particularly for species located at the edges of their latitudinal and altitudinal ranges.  
36 While extensively studied in Central Europe, European beech forests require further  
37 investigation to understand how climate change will affect these ecosystems in  
38 Mediterranean areas. Proposed silvicultural options increasingly aim at sustainable  
39 management to reduce biotic and abiotic stresses and enhance these forest  
40 ecosystems' resistance and resilience mechanisms. Process-based models (PBMs) can  
41 help us to simulate such phenomena and capture early stress signals while considering  
42 the effect of different management approaches. In this study, we focus on estimating  
43 sensitivity of two state-of-the-art PBMs forest models by simulating carbon and water  
44 fluxes at the stand level to assess productivity changes and feedback resulting from  
45 different climatic forcings. Utilizing 3D-CMCC-FEM and MEDFATE models, we  
46 simulated and analyzed carbon (C) and water (H<sub>2</sub>O) fluxes in diverse forest plots under  
47 managed vs. unmanaged scenarios and under current climate and different climatic  
48 forcings (RCP4.5 and RCP8.5), in two sites, on the Italian peninsula, Cansiglio in the  
49 north and Mongiana in the south. To ensure confidence in the models' results, we first  
50 evaluated their performance in simulating C and H<sub>2</sub>O flux in three additional beech  
51 forests along a latitudinal gradient spanning from Denmark to central Italy. The results  
52 from both models for C and H<sub>2</sub>O flux assessment showed generally good model  
53 accuracy. At the Cansiglio site in northern Italy, both models simulated a general  
54 increase in C and H<sub>2</sub>O fluxes under the RCP8.5 climate scenario compared to the  
55 current climate. Still, no benefit in managed plots compared to unmanaged ones, as the  
56 site does not have water availability limitations, and thus, competition for water is low.  
57 At the Mongiana site in southern Italy, both models simulate a decrease in C and H<sub>2</sub>O  
58 fluxes and sensitivity to the different climatic forcings compared to the current climate,

59 with an increase in C and H<sub>2</sub>O fluxes considering specific management regimes  
60 compared to unmanaged scenarios. Conversely, in both models, under unmanaged  
61 scenarios, plots are simulated to experience first signals of mortality prematurely due  
62 to water stress (MEDFATE) and carbon starvation (3D-CMCC-FEM) scenarios. In  
63 conclusion, while management interventions may be considered a viable solution for  
64 the conservation of beech forests under future climate conditions at moister sites like  
65 Cansiglio, in drier sites like Mongiana may not lie in management interventions alone  
66 but rather in the establishment of synergistic mechanisms with other species.

67

68 **Keywords:** Climate change sensitivity, *Fagus sylvatica* L., Forest management  
69 sensitivity, Carbon fluxes, Water fluxes, Stress mitigation, Process-based models.

70

## 71 **1. Introduction**

72 Predicting the future evolution of European forests is essential to continue to benefit  
73 from the ecosystem services they provide for human well-being. Forests offer, for  
74 instance, climate change mitigation through their ability to store atmospheric carbon  
75 dioxide in biomass and soil (Augusto and Bo, 2022; Pan et al., 2024). In 2020, the  
76 European Green Deal prioritized the vital role of forests and the forestry sector in  
77 attaining sustainability objectives, such as promoting sustainable forest management,  
78 enhancing forest resilience, and climate change mitigation (European Commission,  
79 2021). Technological advances and studies of forest ecosystem responses to  
80 management practices continue to promote the evolution of strategies that maintain or  
81 enhance forest ecosystem services, such as promoting biological diversity, water  
82 resources, soil protection, or carbon sequestration (Pukkala, 2016). Different forest  
83 management systems have been adopted in Europe over the years (e.g., clear-cutting  
84 or shelterwood) depending, among others, on the wood product desired, the stand  
85 age, and structure (Brunet et al., 2010).

86 Forest management can be a key element in mitigating the effects of climate warming,  
87 maintaining the current primary productivity and the current distribution of tree  
88 species, or altering forest composition with more suited and productive species (Bosela  
89 et al., 2016). Indeed, the carbon sequestration capacity and productivity of forests are  
90 dependent, primarily, on species composition, site conditions as well as on stand age  
91 (Rötzer et al., 2010; Vangi et al., 2024a, b), which are affected by past and present  
92 forest management activities. According to Collalti et al. (2018) and Dalmonech et al.  
93 (2022), monospecific forests in Europe would appear unable to further increase the  
94 current rates of carbon storage and biomass production in future climate scenarios,  
95 considering current management practices, but at the same time demonstrating that  
96 managing under Business as Usual (BAU) practices still allows forests to accumulate  
97 biomass at higher rates compared to stands left to develop undisturbed.

98 European beech (*Fagus sylvatica* L.) is an important deciduous tree species widely  
99 distributed in Europe, from southern Scandinavia to Sicily and Spain to northwest  
100 Turkey (Durrant et al., 2016). In Italy, according to the National Forest Inventory (INFC,  
101 2015), beech forests cover a total area of 1,053,183 hectares, accounting for about 11.7%  
102 of the country's overall forested land. European beech forests demonstrate  
103 susceptibility to temperature and precipitation fluctuations. For instance, a warmer  
104 environment and less precipitation are forcing shifts in distribution area or the onset of  
105 loss of canopy greenness (Axer et al., 2021; Noce et al., 2017, 2023; Zuccarini et al.  
106 2023; Rezaie et al. 2018). According to Skrk et al. (2023), the decline in growth of the  
107 beech forests primarily occurs in the dry and warm marginal conditions prevalent near  
108 the geographical edge of its distribution with a sub-Mediterranean climatic regime,  
109 posing a threat to the survival of beech populations in those areas. However, tree ring  
110 analyses have also revealed an unexpected increase in growth in the south  
111 Mediterranean region of Albania and Macedonia beech forests at the end of the 20<sup>th</sup>

112 century, challenging the presumed suppression of forest ecosystems due to drought  
113 (Tegel et al., 2014). Puchi et al. (2024) additionally shed light on the susceptibility to  
114 extreme drought events of beech forests found at higher latitudes compared to those  
115 found at lower latitudes in the Italian peninsula by highlighting an increase, for the  
116 latter, in growth related to the abundance of precipitation. In this context, it is  
117 important to minimize the uncertainty surrounding the response of the carbon, water,  
118 and energy cycles within beech forest ecosystems, especially as they have been  
119 shown to adapt to varying environmental drivers (Deb Burman et al., 2024).

120 Process-based models (PBMs) are useful tools for studying forest dynamics, such as  
121 growth and mortality, as well as water (H<sub>2</sub>O) and carbon (C) use efficiency, and carbon  
122 stocks as key variables of forest mitigation potential (Vacchiano et al., 2012; Pilli et al.,  
123 2022; Testolin et al., 2023; Morichetti et al., 2024). For many years, forest modelling has  
124 been widely used by forest ecologists for tackling numerous applied research  
125 questions, and the field is continuously evolving to include increasingly complex  
126 processes to improve model predictions of forest ecosystem responses to changing  
127 climates (Riviere et al., 2020; Kimmins et al., 2008; Maréchaux et al., 2021). By  
128 comparing the predictive performance of different models under current  
129 environmental conditions, it is possible to gain confidence in their predictions of future  
130 trends and make informed decisions in forest ecosystem management and planning  
131 processes (Huber et al., 2013; Mahnken et al., 2022).

132 The main goal of the present study is to investigate the sensitivity of two state-of-the-  
133 science PBMs: 3D-CMCC-FEM (Collalti et al., 2014) and MEDFATE (De Cáceres et al.,  
134 2023). First under different forest management regimes and climate change scenarios  
135 for European beech forests in the Mediterranean area, seeking further insights into the  
136 C and H<sub>2</sub>O fluxes of this species under different management practices and changing  
137 environmental conditions. The study sites vary in terms of environmental factors that

138 can affect gross primary productivity (GPP), as well as latent heat (LE), which are the  
139 two variables considered in this analysis. Specifically, we tested: (i) to what extent  
140 different forest management options can influence C and H<sub>2</sub>O fluxes under the  
141 present-day climate; and, (ii) how harsher climate conditions may affect the C and H<sub>2</sub>O  
142 fluxes under different management options. To address these questions we  
143 parameterized and evaluated model performance for C and H<sub>2</sub>O fluxes at three forest  
144 stands dominated by beech forests: the Sorø (DK-Sor), Hesse (FR-Hes), and Collelongo  
145 (IT-Col) sites, which are included in the PROFOUND Database (PROFOUND DB) (Reyer  
146 et al., 2020a, b). Subsequently, we assessed the C and H<sub>2</sub>O fluxes at two target and  
147 independent beech forest sites in Italy (Cansiglio and Mongiana) by simulating their  
148 development under various management options and evaluating their (model)  
149 sensitivity to current and more severe climate conditions.

150

## 151 **2. Material and Methods**

### 152 **2.1 3D-CMCC-FEM model**

153 The 3D-CMCC-FEM v.5.6 (*Three-Dimensional – Coupled Model Carbon Cycle –*  
154 *Forest Ecosystem Module*) (Collalti et al., 2024 (and references therein); Marconi et al.,  
155 2017; Dalmonch et al., 2022, 2024; Vangi et al., 2024a, 2024b; Morichetti et al., 2024)  
156 is an eco-physiological, biogeochemical and biophysical model. The model simulates C  
157 and H<sub>2</sub>O fluxes occurring within forest ecosystems daily, monthly, or annually,  
158 depending on the processes to simulate, with a common spatial scale of one hectare  
159 (Collalti et al., 2016). Photosynthesis is simulated using the biochemical model of  
160 Farquhar–von Caemmerer–Berry (Farquhar et al., 1980), integrating the sunlit and  
161 shaded leaves of the canopy (De Pury and Farquhar, 1997). For the temperature  
162 dependence of the Michaelis-Menten coefficient for Rubisco and the CO<sub>2</sub>  
163 compensation point without mitochondrial respiration, the model adopts the

164 parameterization described in Bernacchi et al. (2001, 2003). The net balance at the  
165 autotrophic level is represented by net primary production in eq 1:

166

$$167 \qquad \qquad \qquad \text{NPP} = \text{GPP} - R_a \qquad \qquad \qquad (1)$$

168

169 where  $R_a$  includes both maintenance respiration ( $R_m$ ) and growth respiration ( $R_g$ ).  
170 When  $R_m$  exceeds GPP, resulting in a negative NPP, the trees utilize their non-structural  
171 carbon reserves (NSC) (i.e., soluble sugars and starch) to meet the carbon demand  
172 (Collalti et al., 2020a; Merganikova et al., 2019). In deciduous trees, NSC is used to  
173 create new leaves during the bud-burst phase, replenishes during the growing season  
174 under favourable photosynthetic conditions, and finally remobilized in tissues to  
175 prepare for dormancy at the end of the growth phase. The replenishment of non-  
176 structural carbon reserves is prioritized to reach the minimum safety threshold (i.e., 11%  
177 of sapwood dry mass for deciduous trees). Failure to consume almost all reserves may  
178 trigger defoliation mechanisms, or in the case of complete depletion (e.g., during  
179 prolonged stress periods), it may lead to the death of the entire cohort of trees (i.e.,  
180 carbon starvation). The stomatal conductance  $g_s$  is calculated using the Jarvis equation  
181 (Jarvis, 1976). The equation includes a species-specific parameter  $g_{s \max}$  (i.e., maximum  
182 stomatal conductance) controlled by some factors such as light, atmospheric  $\text{CO}_2$   
183 concentration, air temperature, soil water content, vapour pressure deficit (VPD), and  
184 stand age. According to Waring and Running (2007) and Monteith and Unsworth  
185 (2008), the Penman-Monteith equation is used to calculate the latent heat (LE) fluxes of  
186 evaporation as a function of incoming radiation, VPD, and conductances at a daily  
187 scale, summing up the canopy, soil, and snow (if any) latent heat expressed as  $\text{Wm}^{-2}$ .  
188 The 3D-CMCC-FEM accounts for forest stand dynamics, including growth, competition  
189 for light, and tree mortality under different climatic conditions, considering both  $\text{CO}_2$

190 fertilization effects and temperature acclimation (Collalti et al., 2018, 2019; Kattge and  
191 Knorr, 2007). Several mortality routines are considered in the model, such as age-  
192 dependent mortality, background mortality (stochastic mortality), self-thinning  
193 mortality, and the aforementioned mortality due to carbon starvation. In addition to  
194 mortality, biomass removal in 3D-CMCC-FEM results from forest management  
195 practices, such as thinning and final harvest (Collalti et al., 2018, Dalmonch et al.,  
196 2022; Testolin et al., 2023). The required model input data include stand age, average  
197 DBH (Diameter at Breast Height), stand density, and tree height (Collalti et al., 2014).  
198 The soil compartment is represented using one single bucket layer, in which the  
199 available soil water (ASW, in mm) is updated every day considering the water inflows  
200 (precipitation and, if provided, irrigation) and outflows (evapotranspiration, i.e., the sum  
201 of evaporation from the soil and transpiration of the canopy). The remaining water  
202 between these two opposite (in sign) fluxes that exceeds the site-specific soil water  
203 holding capacity is considered lost as runoff. For a full 3D-CMCC-FEM description, see:  
204 <https://doi.org/10.32018/ForModLab-book-2024>.

205

## 206 **2.2 MEDFATE model**

207 MEDFATE v.4.2.0 is an R-based modelling framework that allows the simulation of the  
208 function and dynamics of forest ecosystems, with a specific emphasis on drought  
209 impacts under Mediterranean conditions (De Cáceres et al., 2021, 2023). MEDFATE  
210 calculates energy balance, photosynthesis, stomatal regulation, and plant transpiration  
211 of gas exchange separately at sub-daily steps. Like 3D-CMCC-FEM, MEDFATE also  
212 simulates photosynthesis at the leaf level using the biochemical model of Farquhar-von  
213 Caemmerer-Berry (Farquhar et al., 1980) for sunlit and shaded leaves (De Pury and  
214 Farquhar, 1997). MEDFATE can simulate plant hydraulics and stomatal regulation  
215 according to two different approaches: (a) steady-state plant hydraulics and



216 optimality-based stomatal regulation (Sperry et al., 1998; Sperry et al., 2017); and (b)  
217 transient plant hydraulics including water compartments and empirical stomatal  
218 regulation (Sureau-ECOS; Ruffault et al., 2022). In this work, we took the second  
219 approach, i.e., Sureau-ECOS (Ruffault et al., 2022).

220 The hydraulic architecture of the Sureau-ECOS module comprises arbitrary soil layers.  
221 The rhizosphere contains coarse and fine root biomass calculated for each soil layer.  
222 The total root xylem conductance is determined by factors such as root length (limited  
223 by soil depth), weight, and distribution across the different layers. In addition, the  
224 resistance to water flow is dependent on two plant compartments (leaf and stem, each  
225 composed of symplasm and apoplasm). Overall, plant conductance is defined by the  
226 sum of resistances across the hydraulic network (i.e., soil, stem, and leaves), taking into  
227 account processes such as plant capacitance effects (i.e., the variation of symplasmic  
228 water reservoirs in the stem and leaves) and cavitation flows (i.e., water released to the  
229 streamflow from cavitated cells to non-cavitated cells during cavitation) (Hölttä et al.,  
230 2009). It also considers cuticular transpiration of the stem and leaf flows. Each element  
231 (roots, stem, leaves) of the hydraulic network has a vulnerability curve  $k(\Psi)$ , that  
232 declines as water pressure becomes more negative. The xylem vulnerability curve is  
233 modelled using a sigmoid function, defined by the equation:

234

$$235 \quad k(\Psi) = k_{max}/1 + \exp^{(slope/25) \cdot (\Psi - \Psi_{50})} \quad (2)$$

236

237 where  $k_{max}$  is the maximum hydraulic conductance,  $\Psi_{50}$  is the water potential  
238 corresponding to 50% of conductance, and "slope" is the slope of the curve at that  
239 point.

240 The stem vulnerability curve can be used to determine the proportion of stem  
241 conductance loss ( $PLC_{stem}$ ) associated with vessel embolism. This embolism reduces

242 overall tree transpiration and photosynthesis. Plant hydraulic failure and tree death can  
243 occur if the  $PLC_{stem}$  exceeds the 50% threshold.

244 Gas exchange in the Sureau-ECOS module depends on stomatal conductance (which  
245 depends on light, water availability, and air temperature) and leaf cuticular  
246 conductance, which changes with leaf temperature due to changes in the permeability  
247 of the epidermis. Stomatal regulation, unlike the 3D-CMCC-FEM, follows the Baldocchi  
248 (1994) approach, which allows coupling leaf photosynthesis with water losses. In  
249 addition, a multiplicative factor depending on leaf water potential is used to decrease  
250 stomatal conductance under drought conditions, following a sigmoidal function similar  
251 to stem vulnerability.

252 Soil water balance is computed daily. MEDFATE can consider an arbitrary number of  
253 soil layers with varying depths in which the water movement within the soil follows a  
254 dual-permeability model (Jarvis et al., 1991, Larsbo et al., 2005). Soil water content  
255 ( $\Delta V_{soil}$ , in mm) is calculated taking into account variables such as infiltration, capillarity  
256 rise, deep drainage, saturation effect, evaporation from the soil surface, transpiration of  
257 the herbaceous plant, and woody plant water uptake. A full MEDFATE description is  
258 available at: <https://emf-creaf.github.io/medfatebook/index.html>.

259

### 260 **2.3 Evaluation sites**

261 Model evaluation was performed in three PROFOUND European beech sites, i.e., Sorø  
262 (DK-Sor, Denmark), Hesse (FR-Hes, France), and Collelongo (IT-Col, Italy), in which we  
263 retrieved information on soil texture, soil depth, and stand inventory data of forest  
264 structure for model initialization (Reyer et al., 2020a, b). Moreover, these sites are  
265 equipped with the Eddy Covariance towers (EC; Pastorello et al., 2020) for long-term  
266 continuous monitoring of atmospheric carbon, water, and energy fluxes of the forests  
267 (Fig. 1). The DK-Sor site is located in the forest Lille Bogeskov on the island of Zealand in  
268 Denmark. FR-Hes is situated in the northeastern region of France and lies on the plain

269 at the base of the Vosges Mountains. IT-Col (Selva Piana stand) is a permanent  
270 experimental plot installed in 1991 and situated in a mountainous area of the Abruzzo  
271 region, the centre of Italy.

272 The pedological characterization of soils exhibits distinct variations across the studied  
273 sites. The soil at the DK-Sor site is predominantly classified as either Alfisols or  
274 Mollisols. The FR-Hes site showcases an intermediary nature, displaying characteristics  
275 akin to both luvisols and stannic luvisols. At the IT-Col site, the prevailing soil type is  
276 identified as Humic alisols, according to the USDA soil classification system. Full details  
277 of these sites are reported in Table 1.

278 The variables accounted for in the evaluation were obtained from the Fluxdata website  
279 (<http://fluxnet.fluxdata.org/data/fluxnet2015-dataset/>) from the FLUXNET2015  
280 database (Pastorello et al., 2020). The variables considered are the daily GPP,  
281 estimated from Net Ecosystem Exchange (NEE) measurements and quality checked  
282 using the constant USTAR turbulence correction according to Papale et al. (2006) and  
283 the Latent Heat flux (LE) with energy balance closure correction (i.e., 'LE\_CORR')  
284 (Pastorello et al., 2020).

285

## 286 **2.4 Study sites**

287 The two target sites considered in this study are Cansiglio and Mongiana Forests (Fig. 1)  
288 (De Cinti et al., 2016). Each site consists of nine long-term monitored plots of differently  
289 managed beech stands, with a spatial extension for each area above 3 hectares, for  
290 about 27 hectares of the experimental area. Three different treatments were applied  
291 (see Fig. S1-S2). For each site, three of the nine plots considered were left unmanaged  
292 (i.e., no cutting and leaving the stands to natural development), defined as 'Control'  
293 plots, three plots were managed following the historical shelterwood system  
294 ('Traditional'), and three with innovative cutting ('Innovative'). In Cansiglio, considering

295 the developmental stage of the stand was an establishment cut to open growing space  
296 in the canopy for the establishment of regeneration. The 'Innovative' cutting consisted  
297 of selecting a non-fixed number of scattered, well-shaped trees (the 'candidate trees')  
298 and a thinning of neighbouring competitors to reduce competition and promote better  
299 growth. In Mongiana, 'Traditional' silvicultural treatment was the first preparatory cut to  
300 increase the vitality and health of the intended residual trees in the stand. The  
301 'Innovative' option was the identification of 45–50 as 'candidate trees' per hectare and  
302 removing only direct competitors.

303 The Cansiglio site is situated in a mountainous area in the Veneto region, northern Italy.  
304 Mongiana site is located in a mountainous area in the Calabria region of southern Italy.  
305 The latter shows higher mean annual temperature (MAT, C°) and lower mean annual  
306 precipitation (MAP, mm year<sup>-1</sup>) (i.e., drier conditions) than the Cansiglio site located at  
307 higher latitudes (Table 1). Data on forest structure and soil texture were collected  
308 during the field campaigns conducted in 2011 and 2019 (Cansiglio) and in 2012 and 2019  
309 (Mongiana). At the Cansiglio site, soils are identified as Haplic luvisols, whereas at  
310 Mongiana, the predominant soil classifications consist of Inceptisols and Entisols,  
311 according to the USDA soil classification system. The variables analyzed in these sites,  
312 like in the evaluation sites, were GPP and LE. A summary for these sites is reported in  
313 Table 1.

314

315

316



317

318 Fig 1. Map of the study sites. Red dots represent sites for validating fluxes, while the blue dot signifies  
319 sites designated for management investigation.

320

321

322

323

324

325

326

327

328

329

330

331

332

333

334

335

336

337

338 Table 1. Characteristics of the study sites. The age of the stands refers to 2010. The mean annual  
 339 temperature (MAT) and mean annual precipitation (MAP) for DK-Sor, FR-Hes and IT-Col refer to the  
 340 period evaluated (i.e., 2006–2010 for the Sorø and Collelongo site and 2014–2018 for the Hesse site)  
 341 while for Cansiglio and Mongiana from 2010 to 2022. The sum of precipitation in summer refers to June  
 342 (J), July (J) and August (A) for the same period.

SITE DESCRIPTION					
Variable	Evaluation sites			Managed sites	
	DK-Sor	FR-Hes	IT-Col	Cansiglio	Mongiana
Coordinates (WGS84)	55°49'N, 11°64' E	48°66'N, 7°08'E	41°85'N, 13°59'E	46°02'N, 12°22'E	38°29'N, 16°14'E
Country	Denmar k	France	Italy	Italy	Italy
Altitude (m a.s.l.)	40	305	1500	1300	1300
Area (ha)	1	1	1	27	27
MAT (°C)	8.52	10.27	6.95	6.44	11.01
MAP (mm)	818	853	1075	2219	1701
Slope (%)	-	5	35	12	10
Aspect (°)	0	0	252	135	135
Stand age (yr)	90	45	118	120	90
Summer prec (J-J-A)(mm)	292	205	120	493	141

343

## 344 2.5 Meteorological data

345 For the evaluation sites (i.e., DK-Sor, FR-Hes, IT-Col) observed meteorological data  
 346 were retrieved from the harmonized PROFOUND database (Reyer et al., 2020a, b) and  
 347 Fluxnet database (<https://data.icos-cp.eu/>).

348 For the Mongiana and Cansiglio sites, meteorological data for 2010–2022 were  
 349 obtained at daily temporal resolution from the relevant region's Regional Environmental  
 350 Protection Agencies (ARPAs), which are responsible for monitoring climate variables  
 351 with weather stations. The choice of thermo-pluviometric weather station was based  
 352 on the minimum distance from the study area (between 2 km and 20 km away from  
 353 the study sites, respectively) and on the data availability and integration with other

354 weather stations in the proximity. The Bagnouls–Gausсен graph (Fig. S3) shows the  
355 mean monthly precipitation (mm) and air temperature (°C) recorded for every station  
356 inside the catchment.

357 Climate scenarios used as inputs for two models at the Cansiglio and Mongiana sites,  
358 were from the COSMO-CLM simulation at a resolution of approximately 2.2 km over  
359 Italy (Raffa et al., 2023).

360 The daily variables considered for 3D-CMCC-FEM were mean solar radiation ( $\text{MJ m}^{-2}$   
361  $\text{day}^{-1}$ ), maximum and minimum air temperature (°C), precipitation ( $\text{mm day}^{-1}$ ), and the  
362 mean relative air humidity (%). In contrast, the MEDFATE model uses mean solar  
363 radiation, maximum and minimum air temperature, precipitation, the daily maximum  
364 and minimum relative air humidity, and wind speed ( $\text{m s}^{-1}$ ).

365

## 366 **2.6 Modelling set-up**

367 A set of parameters specific for *Fagus sylvatica* L. was provided as input to the model  
368 3D-CMCC-FEM as described in Collalti et al. (2023) while for MEDFATE as in De  
369 Cáceres et al. (2023). To remove any confounding factors related to parameterization,  
370 the parameters related to photosynthesis and stomatal conductance were kept  
371 constant between the two models (see Table 2). The maximum stomatal conductance  
372 ( $g_{s \text{ max}}$ ) was set for 3D-CMCC-FEM according to Pietsch et al. (2005) as in BIOME BGC  
373 model. In 3D-CMCC-FEM, the maximum RuBisCO carboxylation rate ( $V_{\text{cmax}}$ ) and the  
374 maximum electron transport rate for the RuBP regeneration ( $J_{\text{max}}$ ) at 25°C are corrected  
375 for leaf temperature according to Medlyn et al. (1999) and soil water content as in  
376 Bonan et al. (2011). In MEDFATE, the  $V_{\text{cmax}}$  and  $J_{\text{max}}$  at 25°C are modified according to  
377 Leuning (2002) leaf temperature dependence and modelled according to Medlyn et al.  
378 (1999) and Collatz et al. (1991).

379 We then used the LAI and Available Soil Water (AWS) values obtained from the 3D-  
380 CMCC-FEM outputs as input for running simulations with the MEDFATE model. This

381 allowed us to isolate and evaluate the specific effects of the processes of interest, such  
382 as the influence of NSC on stomatal conductance and photosynthesis, compared to the  
383 impact of hydraulic constraints on these same physiological processes.

384 The LAI values were forced annually from the 3D-CMCC-FEM to the MEDFATE model  
385 since it is currently not possible to prescribe LAI values in the 3D-CMCC-FEM model  
386 (i.e., it is calculated prognostically). Precisely, here we used MEDFATE to simulate C  
387 and H<sub>2</sub>O fluxes only while considering plant hydraulics (De Cáceres et al., 2021), from  
388 the forest structure predicted by 3D-CMCC-FEM. For MEDFATE water balance, LAI  
389 values determine the competition for light and also drive the competition for soil water,  
390 along with the root distribution across soil layers.

391

392 Table 2. Parameters and variables set for both models during the simulations.

PARAMETERS AND VARIABLES		
Name	Value	Unit
$g_{s \max}$	0.006 Pietsch et al. (2005)	m s <sup>-1</sup>
$J_{\max}$	-160 De Cáceres et al. (2023)	μmol photons m <sup>-2</sup> s <sup>-1</sup>
$V_{c\max}$	-95 De Cáceres et al. (2023)	μmol CO <sub>2</sub> m <sup>-2</sup> s <sup>-1</sup>
LAI	from 3D-CMCC-FEM to MEDFATE	m <sup>2</sup> m <sup>-2</sup>
ASW	from 3D-CMCC-FEM to MEDFATE	mm

393

394

## 395 2.7 Model evaluation

396 Both models were run for five years on the evaluation sites, with the simulation period  
397 determined by the availability of observed data provided, as already mentioned, from  
398 the PROFOUND database, specifically, from 2006 to 2010 at DK-Sor and IT-Col sites  
399 while for FR-Hes starting from 2014 to 2018. The performance metrics of the results of  
400 the evaluation for each site for the GPP and LE variables were the coefficient of  
401 determination (R<sup>2</sup>), Root Mean Square Error (RMSE), and Mean Absolute Error (MAE).



402

## 403 **2.8 Model application in managed sites**

404 In the managed sites (i.e., Cansiglio and Mongiana), simulations were performed using  
405 Historical climate ('Hist') and, to analyse models' sensitivities to climate change, under  
406 two Representative Concentration Pathways 4.5 and 8.5 ('Moderate' and 'Hot Climate'),  
407 respectively. The 'Hist' climate was used to run simulations at the Cansiglio site from  
408 2011 to 2022 and the Mongiana site from 2012 to 2022. In contrast, simulations using  
409 RCP4.5 and RCP8.5 climate ran accounting for the same period, that is, 11 years for the  
410 Cansiglio site and ten years for the Mongiana site, but considering the last years of the  
411 climate change scenarios (i.e., 2059–2070 and 2060–2070, respectively) to create  
412 harsher temperature and precipitation conditions, but with an increased atmospheric  
413 CO<sub>2</sub> concentration (in  $\mu\text{mol mol}^{-1}$ ).

414 For each of the nine sampled areas, in the Cansiglio and Mongiana sites, we considered  
415 a representative area of one hectare for each type of plot: 'Control', 'Traditional' , and  
416 'Innovative'. At the beginning of the simulations, each site thus included a total of 9  
417 plots, each one hectare in size—comprising three 'Control' plots, three 'Traditional'  
418 plots, and three 'Innovative' plots. This setup resulted in a total of nine hectares being  
419 simulated per site where the model 3D-CMCC-FEM removed a certain percentage of  
420 the Basal Area (BA) according to the LIFE-ManFor project (see Table S2). 'Traditional'  
421 and 'Innovative' cutting took place for the first time in 2012 (Cansiglio) and 2013  
422 (Mongiana), respectively. Following preliminary results, since the Mongiana site  
423 experienced a lighter thinning intensity compared to the Cansiglio site (refer to Table  
424 S2), consequently, for the Mongiana site, we considered an alternative management  
425 option involving the removal of 40% of the BA. This was done to evaluate whether a  
426 more intensive management approach ('SM') could have influenced models' results on

427 Gross Primary Productivity (GPP) and Latent Heat (LE) fluxes related to the reduction in  
428 competition and enhancing water availability.

429

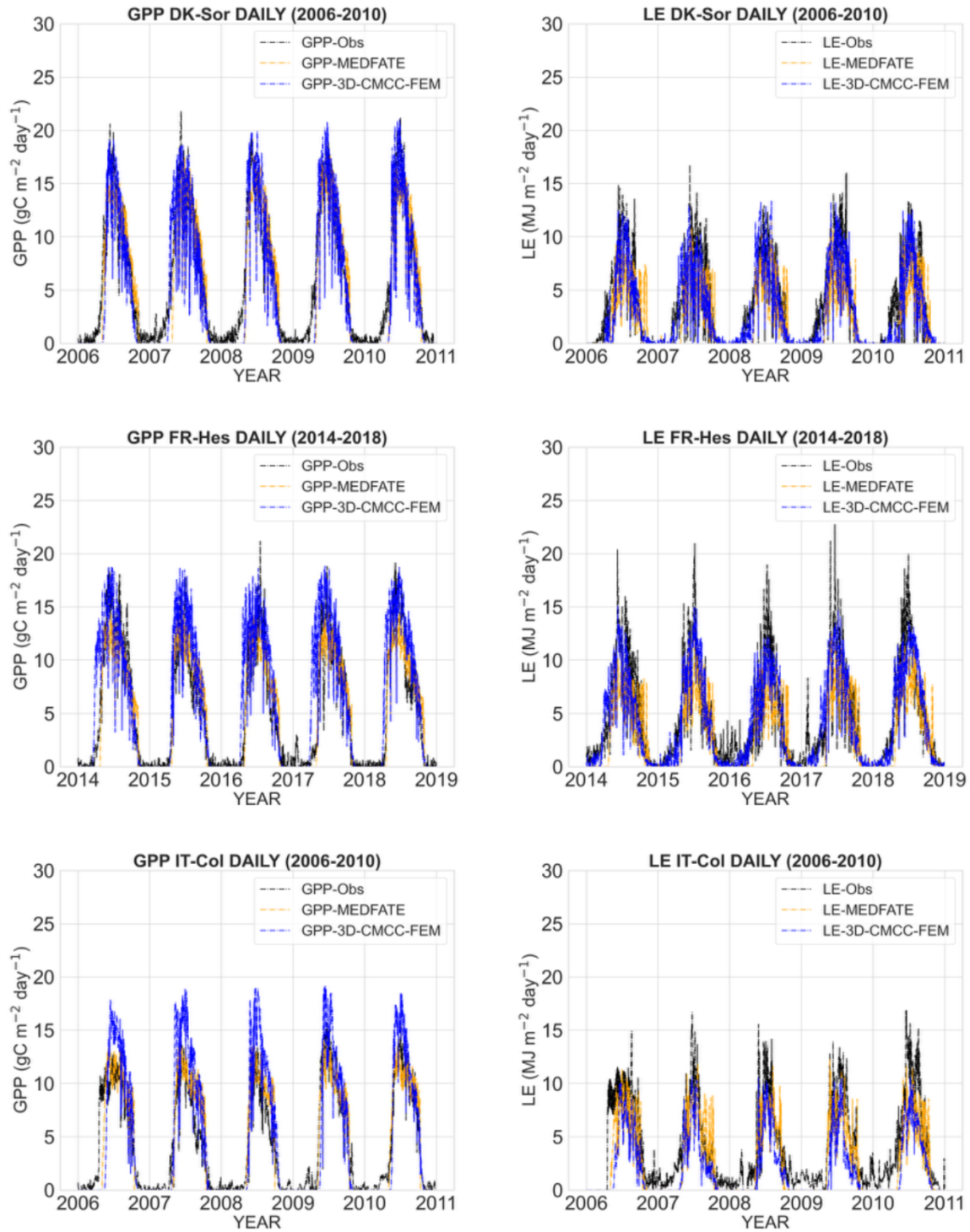
### 430 **3. Results**

#### 431 **3.1 Model evaluation**

432

433 The daily gross primary productivity (GPP) at DK-Sor, FR-Hes, and IT-Col sites was  
434 estimated from EC and simulated by 3D-CMCC-FEM and MEDFATE, are shown in Fig.  
435 2. At DK-Sor site, the 3D-CMCC-FEM simulates a mean daily GPP of  $5.14 \text{ gC m}^{-2} \text{ day}^{-1}$ ,  
436 while MEDFATE  $5.13 \text{ gC m}^{-2} \text{ day}^{-1}$ ; and EC  $5.54 \text{ gC m}^{-2} \text{ day}^{-1}$ ; at the FR-Hes site, 3D-  
437 CMCC-FEM mean daily GPP of  $6.18 \text{ gC m}^{-2} \text{ day}^{-1}$  compared to MEDFATE  $4.82 \text{ gC m}^{-2}$   
438  $\text{day}^{-1}$ , and EC  $4.99 \text{ gC m}^{-2} \text{ day}^{-1}$ ; lastly at the IT-Col site, 3D-CMCC-FEM mean daily  
439 GPP of  $4.88 \text{ gC m}^{-2} \text{ day}^{-1}$  compared to MEDFATE  $4.19 \text{ gC m}^{-2} \text{ day}^{-1}$ ; and EC  $4.11 \text{ gC m}^{-2}$   
440  $\text{day}^{-1}$ ; Additionally, at the DK-Sor site, the 3D-CMCC-FEM mean daily LE to the  
441 atmosphere of  $2.83 \text{ MJ m}^{-2} \text{ day}^{-1}$ , while the MEDFATE mean value of  $2.22 \text{ MJ m}^{-2} \text{ day}^{-1}$ ;  
442 and EC  $3.19 \text{ MJ m}^{-2} \text{ day}^{-1}$ ; at the FR-Hes site, 3D-CMCC-FEM mean daily LE of  $4.16 \text{ MJ}$   
443  $\text{m}^{-2} \text{ day}^{-1}$  compared to MEDFATE  $3.01 \text{ MJ m}^{-2} \text{ day}^{-1}$ ; and EC  $4.47 \text{ MJ m}^{-2} \text{ day}^{-1}$ ; in the  
444 end at the IT-Col site, 3D-CMCC-FEM mean daily LE of  $2.02 \text{ MJ m}^{-2} \text{ day}^{-1}$  compared to  
445 MEDFATE  $2.57 \text{ MJ m}^{-2} \text{ day}^{-1}$ ; while EC  $3.93 \text{ MJ m}^{-2} \text{ day}^{-1}$ . The GPP predicted by 3D-  
446 CMCC-FEM has shown higher values of  $R^2$  (0.92) at DK-Sor and the lowest value at FR-  
447 Hes site ( $R^2 = 0.76$ ) whilst a value of  $R^2 = 0.83$  at IT-Col site, respectively. For the  
448 MEDFATE model, the GPP predicted highest value of  $R^2$  (0.85) was at DK-Sor the  
449 lowest ( $R^2 = 0.68$ ) at IT-Col, and at FR-Hes  $R^2 = 0.76$  the same showed for the 3D-  
450 CMCC-FEM model, respectively. Differently, the highest  $R^2$  (0.89) value for 3D-CMCC-  
451 FEM considering LE predicted vs. observed was at FR-Hes site and almost the same  
452 values for DK-Sor and IT-Col sites ( $R^2 = 0.85$  and  $0.84$ , respectively). MEDFATE, for

453 predicted vs. observed LE variable, has shown the highest  $R^2$  (0.77) at IT-Col site, lower  
454  $R^2$  (0.69) value at FR-Hes site and the lowest  $R^2$  (0.62) value at DK-Sor site,  
455 respectively. In general, both the Root Mean Square Error (RMSE) and Mean Absolute  
456 Error (MAE) values in all sites were reasonably low, falling within the ranges of 3.31 to  
457 2.02  $\text{gC m}^{-2} \text{ day}^{-1}$  and 2.46 to 1.47  $\text{MJ m}^{-2} \text{ day}^{-1}$ , for both models and for both the  
458 variables. In Fig. 3 and Table 3 the summary of the evaluation metrics performance  
459 results.  
460

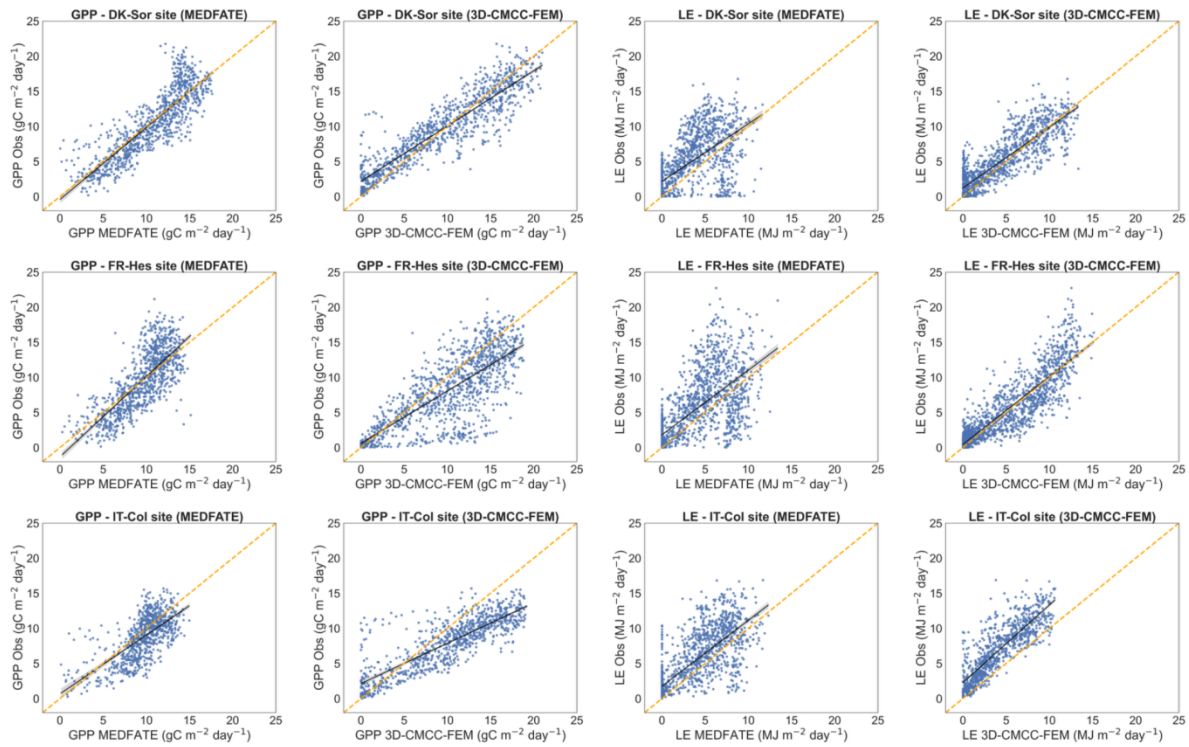


461

462 Fig 2. Daily mean variations of GPP (gC m<sup>-2</sup> day<sup>-1</sup>) and LE (MJ m<sup>-2</sup> day<sup>-1</sup>) estimated from the direct  
463 micrometeorological eddy covariance measurements (GPP-Obs and LE-Obs) and models' simulation  
464 (GPP-3D-CMCC-FEM, LE-3D-CMCC-FEM and, GPP-MEDFATE, LE-MEDFATE) during the evaluation  
465 period at the DK-Sor, IT-Col and FR-Hes at the Beech forest in 2006–2010 and 2014–2018, respectively.

466

467



468

469

Fig 3. Scatter plots and linear regressions of GPP ( $\text{gC m}^{-2} \text{ day}^{-1}$ ) and LE ( $\text{MJ m}^{-2} \text{ day}^{-1}$ ) of the models versus the direct micrometeorological eddy covariance measurements (Obs) at the Sorø (DK-Sor; 2006–2010 period), Collelongo (IT-Col; 2006–2010 period) and Hesse (FR-Hes; 2014–2018 period).

470

471

472

473

474

475

476

477

478

479

480

481

482

483

484

485

486

487

488

489

490

491

492 Table 3. The correlation coefficient ( $R^2$ ), the Root Mean Square Error (RMSE) and the Mean Absolute Error  
 493 (MAE) for, the GPP ( $\text{gC m}^{-2} \text{ day}^{-1}$ ) and LE ( $\text{MJ m}^{-2} \text{ day}^{-1}$ ) of the daily simulations at DK-Sor, IT-Col, and  
 494 FR-Hes sites performed from both models 3D-CMCC-FEM and MEDFATE in the beech forest stands.

	3D-CMCC-FEM						MEDFATE					
	GPP			LE			GPP			LE		
	$R^2$	RMSE	MAE	$R^2$	RMSE	MAE	$R^2$	RMSE	MAE	$R^2$	RMSE	MAE
DK-Sor	0.91	2.17	1.65	0.85	2.02	1.58	0.85	2.52	1.97	0.62	3.09	2.39
FR-Hes	0.76	3.30	2.46	0.89	2.09	1.47	0.76	2.80	2.21	0.69	3.31	2.37
IT-Col	0.83	2.09	1.56	0.84	2.05	1.57	0.68	2.32	1.87	0.77	2.64	1.90

495

496

### 497 3.2 Simulation results at Cansiglio

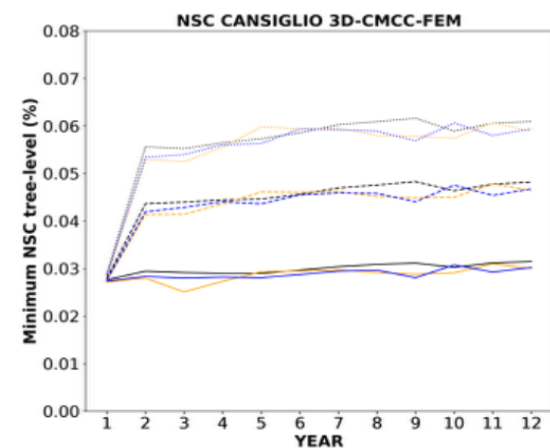
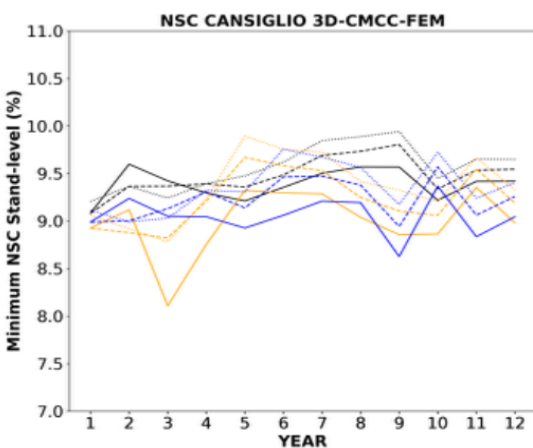
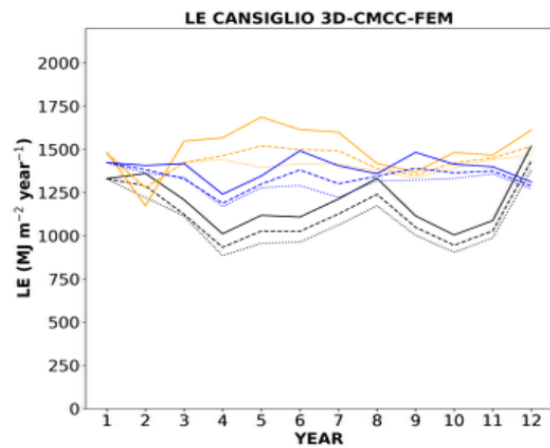
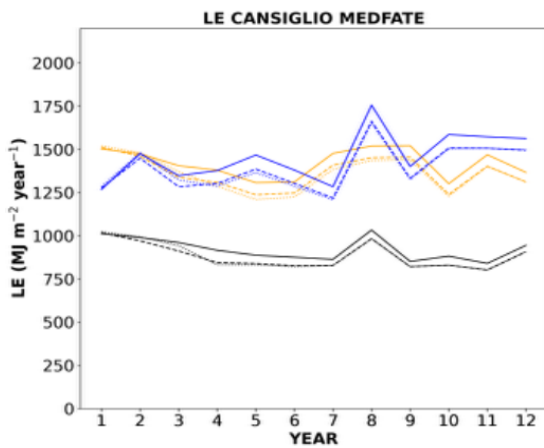
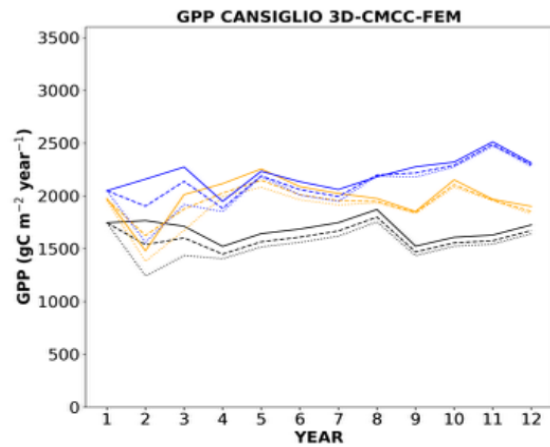
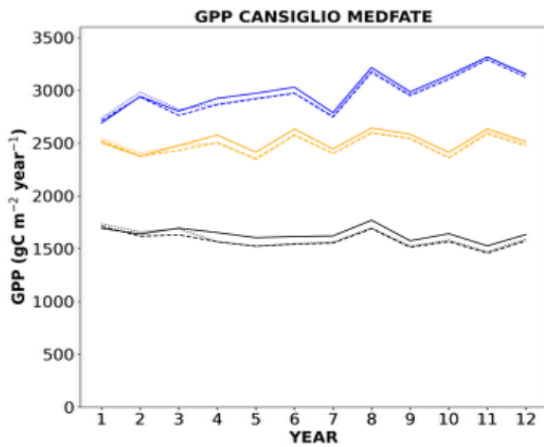
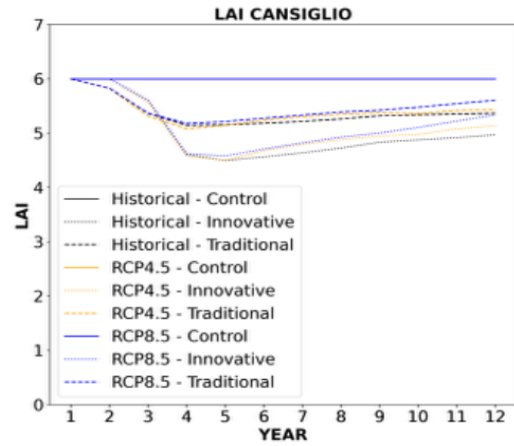
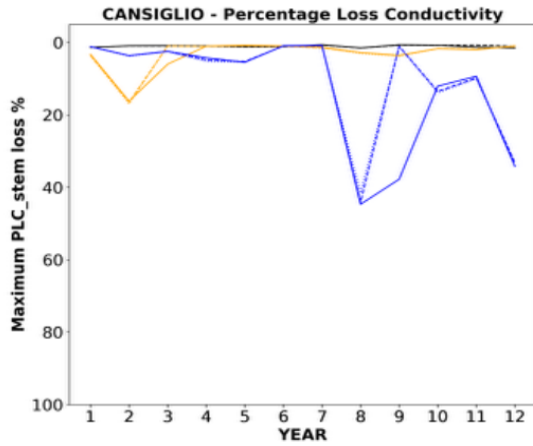
498

499 Fig. 4 shows the simulation results using the 3D-CMCC-FEM and MEDFATE models in  
 500 the Cansiglio site. For the 3D-CMCC-FEM, the 'Control' plot exhibited the lowest GPP  
 501 values under 'Hist' climate conditions, averaging  $1681 \text{ gC m}^{-2} \text{ year}^{-1}$ . These values  
 502 increased slightly to  $1982 \text{ gC m}^{-2} \text{ year}^{-1}$  under the RCP4.5 climate and further rose to  
 503  $2204 \text{ gC m}^{-2} \text{ year}^{-1}$  under the RCP8.5 climate. Similarly, for plots managed with  
 504 'Traditional' methods, the trends were consistent with the 'Control' plot, showing  
 505 average GPP values of 1603, 1942, and  $2141 \text{ gC m}^{-2} \text{ year}^{-1}$  under 'Hist', RCP4.5 and  
 506 RCP8.5 climate, respectively. However, 'Innovative' management showed lower GPP  
 507 fluxes across all three climate scenarios, with average values of 1534, 1882, and 2075  
 508  $\text{gC m}^{-2} \text{ year}^{-1}$  under 'Hist' RCP4.5 and RCP8.5 climate, respectively. The MEDFATE  
 509 model showed higher mean absolute GPP increases than the 3D-CMCC-FEM model

510 under RCP4.5 and RCP8.5 climates, respectively. Under the 'Hist' climate and all  
511 treatments, the mean GPP values were about 1638 gC m<sup>-2</sup> year<sup>-1</sup>, whereas under the  
512 RCP4.5 climate, they rose to 2516 gC m<sup>-2</sup> year<sup>-1</sup> and 2995 gC m<sup>-2</sup> year<sup>-1</sup> under RCP8.5  
513 climate. Analyzing in Fig. 4 the trends of LE for the 3D-CMCC-FEM model, these trends  
514 closely follow those of GPP concerning management treatments. The 3D-CMCC-FEM  
515 LE values for the 'Control' plots, similar to GPP, were lowest for the 'Hist' climate with  
516 an average value over the simulation years of 1200 and 1501 MJ m<sup>-2</sup> year<sup>-1</sup> for the  
517 RCP4.5 climate, and 1391 MJ m<sup>-2</sup> year<sup>-1</sup> for the RCP8.5 climate, respectively. The LE of  
518 the 'Traditional' management predicts values of 1129 in the 'Hist' climate, 1440 in the  
519 RCP4.5 climate, and 1338 MJ m<sup>-2</sup> yr<sup>-1</sup> in the RCP8.5 climate, respectively. For the  
520 'Innovative' management, the mean LE values were 1121 in the 'Hist' climate, 1403 for  
521 the RCP4.5 climate, and 1306 MJ m<sup>-2</sup> yr<sup>-1</sup> for the RCP8.5 climate, respectively. Similar to  
522 the GPP fluxes, the MEDFATE model simulated reductions in LE fluxes among the  
523 treatments and higher values across the climates. The mean LE value modelled in the  
524 'Hist' climate, grouped by treatments (because of slight differences among  
525 managements), was about 920, 1419 in the RCP4.5 climate, and 1456 MJ m<sup>-2</sup> yr<sup>-1</sup> in the  
526 RCP8.5 climate, respectively. MEDFATE simulated a stem xylem conductance loss of  
527 approximately 40% in the seventh, eighth, and twelfth years of simulation for the  
528 RCP8.5 climate scenario in the 'Control' plot. In contrast, this loss was predicted only in  
529 the seventh year for the managed plots. Conversely, near-zero or negligible stem  
530 embolism were simulated under the 'Hist' and RCP4.5 climate scenarios. The 3D-  
531 CMCC-FEM simulated higher values, albeit in a small percentage (i.e., between 8-10%)  
532 of NSC, increasing proportionally to the intensity of basal area removed, better  
533 observable in the graph at the tree level.

534

535



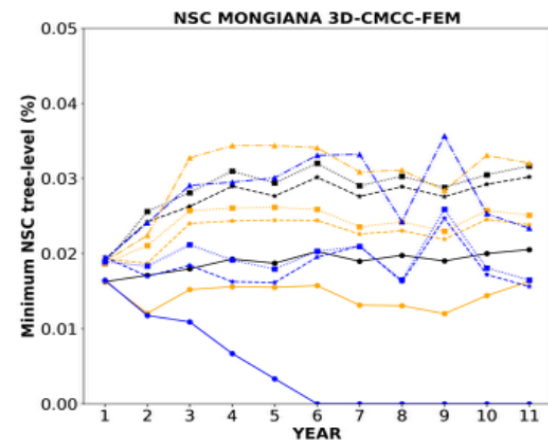
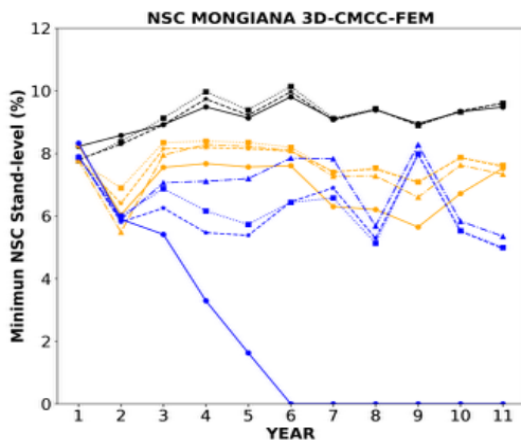
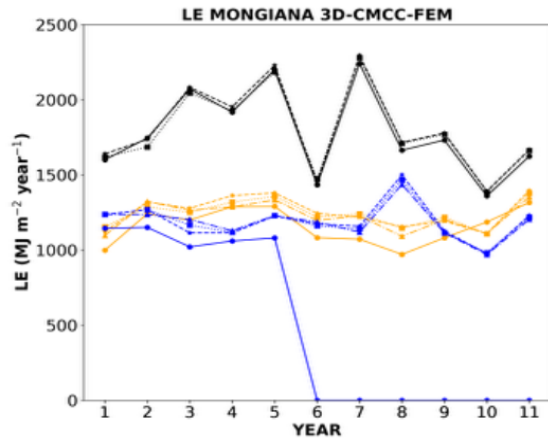
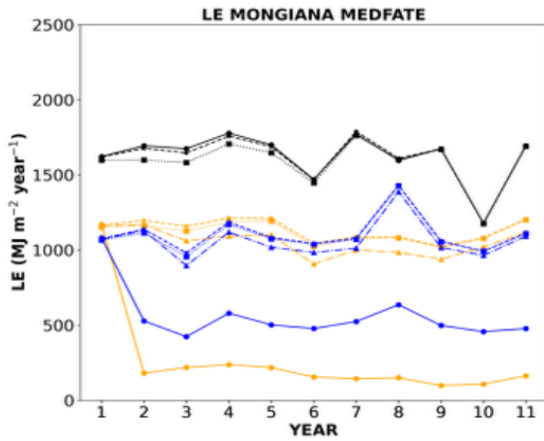
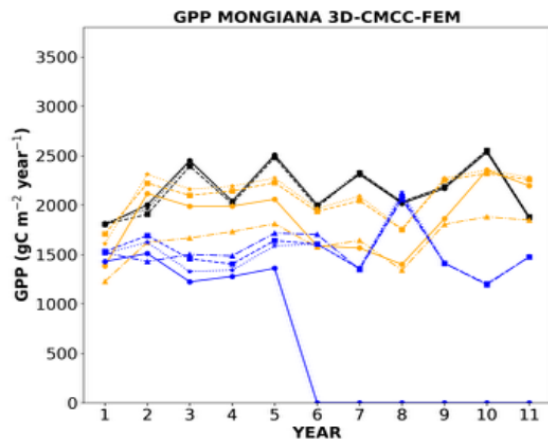
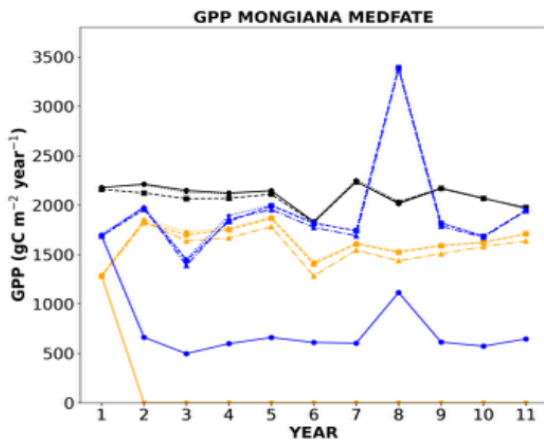
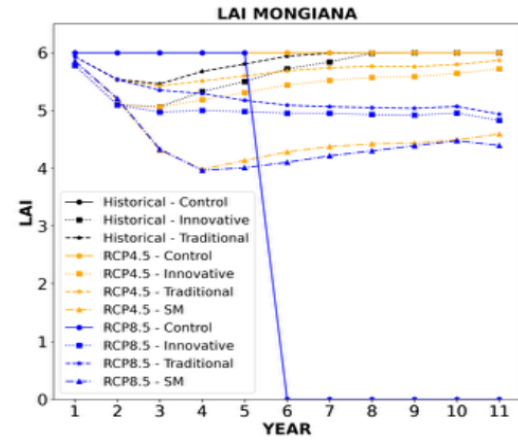
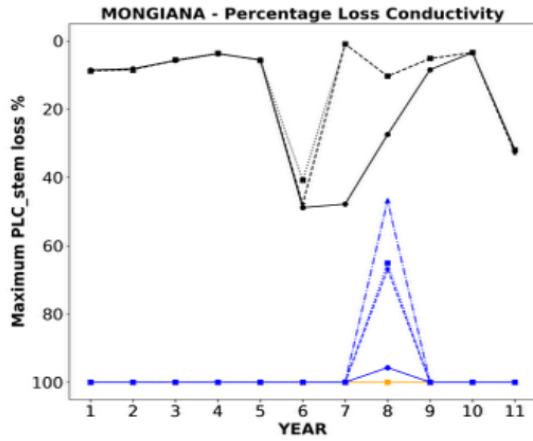


537 Fig 4. Comparative analysis between models output at the Cansiglio site. The top-left panel displays the  
538  $PLC_{stem}$  as modelled by MEDFATE, while the top-right panel shows the modelled LAI for 3D-CMCC-FEM  
539 (and used by MEDFATE). The middle-up panels (left and right) present annual GPP ( $gC\ m^{-2}\ year^{-1}$ ) as  
540 modelled by the MEDFATE and 3D-CMCC-FEM, respectively. The middle-down panels (left and right)  
541 depict annual LE ( $MJ\ m^{-2}\ yr^{-1}$ ) modelled by the MEDFATE and 3D-CMCC-FEM, respectively. The bottom  
542 panels (left and right) depict the annual minimum of NSC concentration (%) at the stand and tree level,  
543 respectively, as modelled by the 3D-CMCC-FEM. Different plot management strategies are represented  
544 by distinct line styles: solid lines for 'Control' plots ('no management'), dotted lines for 'Innovative' plots,  
545 and dashed lines for 'Traditional' plots (Shelterwood). Climate scenarios are indicated by line colours:  
546 black for 'Hist' climate data (2010–2022), orange and blue for RCP4.5 and RCP8.5 climate (2059–2070),  
547 respectively.  
548  
549

### 550 3.3 Simulation results at Mongiana

551 Simulation results at the (drier) Mongiana site well depicted the differences with the  
552 rainy Cansiglio site (Fig. 5). The 3D-CMCC-FEM model showed no significant  
553 differences in the mean values of GPP among various management interventions under  
554 'Hist' climate conditions, with a mean value of  $2151\ gC\ m^{-2}\ yr^{-1}$ . Compared to the  
555 Cansiglio site, Mongiana exhibited lower average GPP values. Under RCP4.5 climate  
556 conditions, the GPP for the 'Control' plot was  $1864\ gC\ m^{-2}\ yr^{-1}$ . In contrast, under the  
557 current climate, the 'Traditional' and 'Innovative' management interventions yielded  
558 higher average GPP values of  $2115\ gC\ m^{-2}\ yr^{-1}$  and  $2086\ gC\ m^{-2}\ yr^{-1}$ . The GPP values  
559 under the more intensive management ('SM') and RCP4.5 climate decreased even  
560 further than those of the 'Control' plot, with an average value of  $1650\ gC\ m^{-2}\ yr^{-1}$ .  
561 Under the RCP8.5, no differences in GPP were observed among management  
562 strategies, with values of about  $1525\ gC\ m^{-2}\ yr^{-1}$ . Moreover, under the RCP8.5, the  
563 'Control' plot experienced complete mortality after five years of simulations. The  
564 MEDFATE model predicted slightly higher average values of GPP in the 'Control' plots  
565 ( $2099\ gC\ m^{-2}\ yr^{-1}$ ) compared to the managed plots ( $2087\ gC\ m^{-2}\ yr^{-1}$ , encompassing  
566 both 'Traditional' and 'Innovative' of two management strategies), with no significant

567 differences observed among the management strategies and under 'Hist' climate.  
568 Under the RCP4.5 and RCP8.5, the GPP values were  $1608 \text{ gC m}^{-2} \text{ yr}^{-1}$  and  $1935 \text{ gC m}^{-2}$   
569  $\text{yr}^{-1}$ , respectively. The  $\text{PLC}_{\text{stem}}$  graph in Fig. 5 indicated very high xylem embolism levels  
570 (i.e., reaching 100% every year) under RCP4.5 and RCP8.5 already in the first year of  
571 simulations. A pronounced embolism event was observed under the 'Hist' climate in  
572 2017, 2018, 2019, and 2022 in a 30–45% range for the 'Control' plots, while the  
573 managed plots experienced a maximum embolism of approximately 40% in 2017.  
574 Conversely, the 3D-CMCC-FEM model did not report any significant differences  
575 between managed and unmanaged plots for the LE. The average LE value for the 'Hist'  
576 climate was  $1796 \text{ MJ m}^{-2} \text{ yr}^{-1}$ , which decreased to  $1220 \text{ MJ m}^{-2} \text{ yr}^{-1}$  under the RCP4.5  
577 and  $1190 \text{ MJ m}^{-2} \text{ yr}^{-1}$  under the RCP8.5 in managed plots. As previously described, the  
578 'Control' plot under the RCP8.5 experienced mortality in the sixth year of simulation.  
579 Similarly to the previously described GPP fluxes, the MEDFATE model reported a slight  
580 difference in LE fluxes between the 'Control' plot under historical climate conditions  
581 ( $1623 \text{ MJ m}^{-2} \text{ yr}^{-1}$ ) and the managed plots ( $1603 \text{ MJ m}^{-2} \text{ yr}^{-1}$ ). For the RCP4.5 and  
582 RCP8.5, the LE values were  $1100 \text{ MJ m}^{-2} \text{ yr}^{-1}$  and  $1089 \text{ MJ m}^{-2} \text{ yr}^{-1}$ , respectively. The LE  
583 values of the 'Control' plots are not reported neither for RCP4.5 nor for RCP8.5 because  
584 of the mortality experienced for the simulation years.  
585



587 Fig 5. Comparative analysis between models output at the Mongiana site. The top-left panel displays the  
588 percent loss of  $PLC_{stem}$  as modelled by MEDFATE while the top-right panel shows the modelled LAI for  
589 3D-CMCC-FEM (and used by MEDFATE). The middle-up panels (left and right) present annual GPP ( $gC$   
590  $m^{-2} year^{-1}$ ) as modelled by the MEDFATE and 3D-CMCC-FEM, respectively. The middle-down panels  
591 (left and right) depict annual LE ( $MJ m^{-2} yr^{-1}$ ) modelled by the MEDFATE and 3D-CMCC-FEM,  
592 respectively. The bottom panels (left and right) depict the annual minimum of NSC concentration (%) at  
593 the stand and tree level, respectively, as modelled by the 3D-CMCC-FEM. Different plot management  
594 strategies are represented by distinct line styles: solid lines with circles for 'Control' plots ('no  
595 management'), dotted lines with squares for 'Innovative' plots, dashed lines with stars for 'Traditional'  
596 plots (Shelterwood) and dash-dotted lines with triangles for 'SM' management. Climate scenarios are  
597 indicated by line colours: black for 'Hist' climate data (2010-2022), orange and blue for RCP4.5 and  
598 RCP8.5 climate (2060-2070), respectively.

599  
600

#### 601 4. Discussion

602 First, this study evaluated the performance of two different process-based models in  
603 simulating different beech stands across Europe, starting to the north of Europe and  
604 moving towards the south under different environmental conditions. Secondly, the  
605 study focused on models' sensitivity to management and different management  
606 options and considering different climatic conditions in two specific beech forest  
607 stands in the north and south of the Italian peninsula.

#### 608 4.1 Model evaluation

609 To assess the models' accuracy in predicting C and  $H_2O$  fluxes, we compared the GPP  
610 and the LE data obtained from the EC towers. Both models predicted GPP and LE  
611 accurately and ensured a good range of general applicability of both models (Kramer et  
612 al., 2002, Verbeeck et al., 2008). The 3D-CMCC-FEM model seems to slightly  
613 overestimate GPP daily values along latitudinal gradients starting from the north (DK-  
614 Sor) to the south (IT-Col), as already found in Collalti et al. (2016). MEDFATE, in  
615 contrast, showed a slight overestimation of GPP only at IT-Col site. The LE predicted by  
616 3D-CMCC-FEM is more accurate than MEDFATE prediction for DK-Sor and FR-Hes  
617 sites but not in IT-Col site in which 3D-CMCC-FEM has shown to underestimate

618 compared to the observed EC values. For MEDFATE the underestimation of LE was  
619 observed in all the evaluation sites.

620 The spread observed for the GPP and LE fluxes between the two models may be  
621 attributed to the different assumptions that govern stomatal regulation since both  
622 models use the Farquhar-von Caemmerer-Berry biochemical model to calculate  
623 photosynthesis. The over or underestimation of the flows estimated by the models  
624 both for GPP and the LE compared to the data observed from the EC towers can be  
625 attributed either to the presence of the understory (although commonly sporadic in  
626 mature beech stands), which was not considered in the simulations by both models  
627 and to errors on daily measurement by EC technique (Loescher et al., 2006) or  
628 because a not perfect fit in the modeled seasonality (i.e., the begin and the end of the  
629 growing season) (Richardson et al., 2010). However, the leaf phenological pattern of  
630 the European beech in these sites is well represented by the two models in almost all  
631 of the years according to EC data as shown in supplementary materials (see Fig. S4, S5,  
632 S6, S7, S8, S9, and Fig S10). It is important to note that we did not specifically calibrate  
633 the model parameters from the eddy covariance data for each site. Instead, as Dufrêne  
634 et al. (2005) already did, both models were parameterized using existing literature  
635 values and with one set of parameter values for all sites.

636

#### 637 **4.2 Climate change and forest management at the Cansiglio and Mongiana site**

638 The pre-Alpine site of Cansiglio showed slight differences in the fluxes (i.e., GPP and LE)  
639 between three different management practices and the three climates used. Future  
640 climate is expected to be higher temperature if compared to the historical one, with  
641 MAT higher of about 3.93°C under RCP4.5 and 4.95°C under RCP8.5 for the Cansiglio  
642 site and 4.52°C under RCP4.5 and 5.42°C under RCP8.5 at the Mongiana site. Similarly,  
643 MAP is expected to be 510 mm lower under RCP4.5 and 602 mm lower under RCP8.5

644 at the Cansiglio site, while 902 mm lower under RCP4.5 and 914 mm lower under  
645 RCP8.5 at the Mongiana site.

646 Regarding management, the response of the 3D-CMCC-FEM to the removal of a  
647 percentage of the basal area from the stand led to a decrease in GPP in the 'Traditional'  
648 cutting and an even greater extent, in the 'Innovative' cutting compared to the 'Control'  
649 (i.e., no management). Similarly to 3D-CMCC-FEM, the MEDFATE model simulates  
650 slight differences in fluxes amount (e.g., lower values for 'Traditional' and 'Innovative'  
651 cutting than 'Control' plots) between the management regimes in the plots. These  
652 results align with those of Guillemot et al. (2014), who observed a slight decrease in  
653 GPP in managed compared to unmanaged temperate beech forests in France under  
654 different thinning regimes. However, differences were observed in both models under  
655 the three different climates used in the simulations. GPP increased from the 'Hist'  
656 climate to RCP4.5 and reached the maximum for RCP8.5, respectively. This suggests a  
657 plastic response (e.g., photosynthesis and stomatal response) of the stands, as  
658 simulated by models, to harsher conditions, indicating, potentially, a high drought  
659 acclimation capacity (Petrik et al., 2022) and increased GPP because of the so-called  
660 'atmospheric CO<sub>2</sub> fertilization' effect as also found by de Wergifosse et al. (2022) and  
661 Reyer et al. (2013), especially in sites with no apparent water limitation both under  
662 current and projected future climate conditions. The anisohydric behavior of *Fagus*  
663 *sylvatica* L. results in prolonged stomatal opening relative to isohydric species,  
664 although Puchi et al. (2024) recently found large variability in European beech  
665 responses, maintaining prolonged photosynthetic activity, though this response is  
666 modulated by summer precipitation and the availability of soil water storage  
667 (Leuschner et al., 2021; Baudis et al., 2015). However, for high-altitude stands, growth  
668 could be negatively affected under warmer conditions, as suggested by Chmura et al.  
669 (2024). The LE results for the 3D-CMCC-FEM showed lower values over the simulation

670 period for managed stands than unmanaged ones showing lesser sensitivity to forest  
671 management if compared to MEDFATE. However, under the RCP4.5, the LE values  
672 were higher compared to both the 'Hist' climate and the RCP8.5 one due to greater  
673 annual cumulative precipitation than the RCP8.5 and higher, on average, temperatures  
674 than the 'Hist' scenario.

675 Conversely, the MEDFATE model was shown to be more sensitive to climate, with a  
676 clearer distinction between the 'Hist' climate, the RCP4.5 and RCP8.5 climates, with  
677 higher and nearly equal values in the harsher conditions (i.e., RCP4.5 and RCP8.5  
678 climates), with slight differences in the management treatments as obtained by 3D-  
679 CMCC-FEM. The Non-Structural carbon (NSC) amount showed the highest values in  
680 'Innovative' plots, followed by 'Traditional' plots, and the lowest values in 'Control'  
681 plots, suggesting a benefit in carbon stock accumulation with more carbon going for  
682 carbon biomass and less for reserve-replenishment for these stands under  
683 management interventions. However, NSC levels remain nearly the same for the three  
684 climate scenarios throughout all the simulation years. It is important to note that  
685 MEDFATE simulated an initial loss of stem conductance under the climate scenarios,  
686 indicating the onset of water stress for the stand. Although in RCP4.5 this is negligible,  
687 in RCP8.5  $PLC_{stem}$  values reach a maximum xylem cavitation value of about 40% in the  
688 eighth year of simulation for managed plots while for 'Control' plots in the eighth, ninth,  
689 and twelfth years, highlighting potential benefits of management to reduce drought  
690 stress (Giuggiola et al., 2018; Schmied et al., 2023).

691 The GPP at the southern Apennine site of Mongiana showed a decrease under RCP4.5  
692 and RCP8.5 scenarios when simulated by the 3D-CMCC-FEM model as a result of  
693 harsher environmental conditions, as also resulted in the study by Yu et al. (2022), in  
694 which the productivity and then the growth of European beech in southern regions are  
695 expected to decrease as affected by more severe climate conditions such as decreased

696 precipitation and increased in air temperature (Tognetti et al., 2019). Indeed, the  
697 increase in air temperature, a reduction in soil water availability, and the rise in vapor  
698 pressure deficit (VPD) lead to earlier stomatal closure, increased mesophyll resistance,  
699 and elevated abscisic acid production (Kane and McAdam, 2023), all of which  
700 contribute to a decrease in the carbon assimilation rate (Priwitzer et al., 2014; Grossiord  
701 et al., 2020). Specifically, GPP is higher under 'Hist' climate conditions, decreases under  
702 the RCP4.5, and ultimately reaches even lower values under the RCP8.5. Under the  
703 RCP8.5 at the fifth year of simulation, the stand in the 'Control' plot is simulated to die  
704 due to carbon starvation. The annual decline in NSC (Fig. 5) due to an imbalance  
705 between carbon uptake (photosynthesis) and the demands for growth and respiration  
706 suggests that the trees are unable to replenish their carbon reserves. The depletion of  
707 NSC reserves may ultimately disrupt processes such as osmoregulation and phenology  
708 (Martínez-Vilalta et al., 2016), potentially leading to stand defoliation and/or mortality.  
709 The management options did not show changes in GPP under the 'Hist' climate.  
710 However, the increase of GPP was observed under the RCP4.5 in the plots where  
711 'Innovative' and 'Traditional' cutting occurred, although no differences were observed  
712 between them. For instance, the same increase in GPP was reported by Fibbi et al.  
713 (2019) for beech forest under climate change scenarios in Italy. The thinning reduces  
714 the LAI and increase the soil water availability, which positively influence stomatal  
715 conductance and carbon assimilation, providing an acclimation mechanism to drought  
716 during periods of water scarcity (Lüttschwager and Jochheim, 2020; Diaconu et al.,  
717 2017).

718 In contrast, the more intense cutting exhibited even lower GPP values than the 'Control'  
719 plots. This is likely due to the overly intense thinning, which contrasts the microclimate  
720 effects within this forest stand, reducing the potential to offset climate warming at the  
721 local scale (Rita et al., 2021). Heavy thinning, on the other hand, can increase light



722 penetration, soil evaporation, and wind speed, thereby heightening tree sensitivity to  
723 vapor pressure deficit under dry conditions (Schmied et al., 2023; Simonin et al., 2007).  
724 LE decreased with the decrease in precipitation under the RCP4.5 and RCP8.5 climate  
725 scenarios compared to the 'Hist' climate. There were no significant differences in LE  
726 among the various management regimes. For the MEDFATE model, negligible or no  
727 differences in GPP were observed under all the climates among various management  
728 options. Although the GPP values estimated by the MEDFATE model under the RCP4.5  
729 and RCP8.5 are similar to those obtained from the 3D-CMCC-FEM model, a closer  
730 analysis of the daily outputs (data not shown) reveals that trees photosynthesize until  
731 the end of July, after which they experience significant embolism (i.e., maximum value  
732 of 100%), as indicated by the  $PLC_{stem}$  graph, indicating that the decrease in  
733 precipitation led to summer soil moisture depletion and lethal drought stress levels.  
734 Furthermore, the 'Control' plots experienced mortality even before reaching the  
735 summer period. In recent decades, prolonged drought stress in Mediterranean  
736 mountain regions has significantly reduced the productivity of beech forests, resulting  
737 in a decline in Basal Area Increment (BAI) and overall growth (Piovesan et al., 2008). It  
738 is also important to note that under 'Hist' climate conditions, the MEDFATE model  
739 indicated a stem embolization loss ranging from approximately 10% to 45% during the  
740 drought period (i.e., 2018–2020) in Europe (Italiano et al., 2024; Thom et al., 2023,  
741 Lombardi et al., 2023). The embolization was more pronounced and long-lasting in the  
742 'Control' plots than the managed ones. The same trends were obtained for LE.

743

## 744 **5. Conclusion**

745 These two process-based models provide robust evidence for their application in  
746 estimating fluxes, consistent with long-term EC tower measurements in European  
747 beech forests. Despite the minimal parametrization effort to align the two models and  
748 the avoidance of site-specific parameters, reliable results can still be obtained, as

749 confirmed by the outputs from the Sorø, Hesse, and Collelongo sites. Regarding the  
750 sub-Alpine Cansiglio site, although water limitation does not significantly impact fluxes  
751 or the health of the forest under Moderate climate conditions (RCP4.5), a potential  
752 concern is the embolization predicted by the MEDFATE model under the Hot climate  
753 (RCP8.5) at this site, despite similar levels of precipitation. The high susceptibility of  
754 beech forests at the southern Apennine site of Mongiana to more severe (i.e., hotter  
755 and drier) climatic conditions could lead to the collapse of this forest ecosystem, even  
756 with the application of management options to reduce competition. This necessitates  
757 strategic management planning, including the ability to project (e.g., with forest  
758 models) and evaluate future forest conditions for better management schemes (Taylor  
759 et al., 2009). However, the ability of these forests to survive or resist the impacts of  
760 climate change may not depend solely on density reduction interventions. Prioritizing  
761 the exploration of alternative sustainable management strategies to promote carbon  
762 sequestration in both above-ground biomass and soil is crucial for enhancing climate  
763 change mitigation efforts. Additionally, evaluating silvicultural plans such as the  
764 introduction of complementary species can improve the resilience of vulnerable beech  
765 ecosystems. A modeling approach, similar to the one used in this study, offers a  
766 valuable tool for assessing these alternative strategies and refining forestry  
767 management practices. By integrating these approaches, we can strengthen the long-  
768 term sustainability of forests while preserving the ecological balance of vulnerable  
769 regions.

770

771

772

773

774

775 **CRedit authorship contribution statement**

776 **Vincenzo Saponaro:** Conceptualization, Data curation, Formal analysis, Investigation,  
777 Methodology, Resources, Software, Visualization, Writing – original draft, Writing –  
778 review & editing. **Miquel De Càceres:** Conceptualization, Methodology, Software,  
779 Supervision, Writing – review & editing. **Daniela Dalmonech:** Conceptualization,  
780 Methodology, Software, Supervision, Writing – review & editing. **Ettore D’Andrea:**  
781 Resources, Methodology, Data curation, Writing – review & editing. **Elia Vangi:**  
782 Resources, Writing – review & editing. **Alessio Collalti:** Conceptualization,  
783 Methodology, Resources, Software, Supervision, Project administration, Writing –  
784 review & editing.

785 **Declaration of Competing Interest**

786 The authors declare that they have no known competing financial interests or personal  
787 relationships that could have appeared to influence the work reported in this paper.

788 **Data availability**

789 Data will be made available on request.

790 **Acknowledgements**

791 We would like to thank the University of Tuscia, the CNR ISAFOM of Perugia and the  
792 company ENI s.p.a. for the realization of this work. Special thanks to the Institute  
793 Research Center for Ecological and Forestry Applications (CREAF) of Barcelona that  
794 supported the research by the Spanish “Ministerio de Ciencia e Innovación”  
795 (MCIN/AEI/10.13039/501100011033) (grant agreement No. PID2021-126679OB-I00).  
796 The authors sincerely thank the ARPA Veneto and Calabria for providing the  
797 meteorological data. The Fondazione Centro Euro-Mediterraneo sui Cambiamenti

798 Climatici (CMCC) for providing climate change scenarios. The Cost-Action PROFOUND  
799 for providing both the stand ancillary data and the climate used in this work. D.D., E.V.  
800 and A.C. has been partially supported by MIUR Project (PRIN 2020) “Unraveling  
801 interactions between WATER and carbon cycles during drought and their impact on  
802 water resources and forest and grassland ecosystems in the Mediterranean climate  
803 (WATERSTEM)” (Project number: 20202WF53Z), “WAFER” at CNR (Consiglio Nazionale  
804 delle Ricerche) and by PRIN 2020 (cod. 2020E52THS) – Research Projects of National  
805 Relevance funded by the Italian Ministry of University and Research entitled: “Multi-  
806 scale observations to predict Forest response to pollution and climate change”  
807 (MULTIFOR, project number: 2020E52THS). D.D., E.V., A.C. acknowledge also funding  
808 by the project OptForEU Horizon Europe research and innovation programme under  
809 grant agreement No. 101060554. D.D. and A.C. also acknowledge the project funded  
810 under the National Recovery and Resilience Plan (NRRP), Mission 4 Component 2  
811 Investment 1.4 – Call for tender No. 3138 of 16 December 2021, rectified by Decree  
812 n.3175 of 18 December 2021 of Italian Ministry of University and Research funded by the  
813 European Union – NextGenerationEU under award Number: Project code  
814 CN\_00000033, Concession Decree No. 1034 of 17 June 2022 adopted by the Italian  
815 Ministry of University and Research, CUP B83C22002930006, Project title “National  
816 Biodiversity Future Centre – NBFC”. This work used eddy covariance data acquired and  
817 shared by the FLUXNET community, including these networks: AmeriFlux, AfriFlux,  
818 AsiaFlux, CarboAfrica, CarboEuropeIP, CarboItaly, CarboMont, ChinaFlux, Fluxnet-  
819 Canada, GreenGrass, ICOS, KoFlux, LBA, NECC, OzFlux-TERN, TCOS-Siberia, and  
820 USCCC. The 3D-CMCC-FEM model code is publicly available and can be found on the  
821 GitHub platform at: <https://github.com/Forest-Modelling-Lab/3D-CMCC-FEM>. The  
822 MEDFATE model code is publicly available and can be found on the GitHub platform at:  
823 <https://github.com/emf-creaf/medfate>.

824

## 825 References

- 826 Augusto, L., Boča, A. (2022). *Tree functional traits, forest biomass, and tree species*  
827 *diversity interact with site properties to drive forest soil carbon*. *Nat. Commun.* 13,  
828 1–12. <https://doi.org/10.1038/s41467-022-28748-0>
- 829 Axer, M., Schlicht, R., Kronenberg, R., Wagner, S. (2021). *The Potential for Future Shifts*  
830 *in Tree Species Distribution Provided by Dispersal and Ecological Niches: A*  
831 *Comparison between Beech and Oak in Europe*. *Sustainability*, 13, 13067.  
832 <https://doi.org/10.3390/su132313067>
- 833 Baldocchi, D. (1994). *An analytical solution for coupled leaf photosynthesis and*  
834 *stomatal conductance models*. *Tree Physiology*, 14(7–8–9), 1069–1079.  
835 <https://doi.org/10.1093/treephys/14.7-8-9.1069>
- 836 Baudis, M., Premper, T., Welk, E., & Bruelheide, H. (2015). *The response of three Fagus*  
837 *sylvatica L. provenances to water availability at different soil depths*. *Ecological*  
838 *Research*, 30(5), 853–865. <https://doi.org/10.1007/s11284-015-1287-x>
- 839 Bernacchi, C. J., Singsaas, E. L., Pimentel, C., Portis, A. R., & Long, S. P. (2001). *Improved*  
840 *temperature response functions for models of Rubisco-limited photosynthesis*.  
841 *Plant Cell & Environment*, 24(2), 253–259. [https://doi.org/10.1111/j.1365-](https://doi.org/10.1111/j.1365-3040.2001.00668.x)  
842 [3040.2001.00668.x](https://doi.org/10.1111/j.1365-3040.2001.00668.x)
- 843 Bernacchi, C. J., Calfapietra, C., Davey, P. A., Wittig, V. E., Scarascia-Mugnozza, G. E.,  
844 Raines, C. A., & Long, S. P. (2003). *Photosynthesis and stomatal conductance*  
845 *responses of poplars to free-air CO<sub>2</sub> enrichment (PopFACE) during the first*  
846 *growth cycle and immediately following coppice*. *New Phytologist*, 159(3), 609–  
847 621. <https://doi.org/10.1046/j.1469-8137.2003.00850.x>
- 848 Bosela, M., Štefančík, I., Petráš, R., Vacek, S. (2016). *The effects of climate warming on*  
849 *the growth of European beech forests depend critically on thinning strategy and*  
850 *site productivity*. *Agric. For. Meteorol.* 222, 21–31.  
851 <https://doi.org/10.1016/j.agrformet.2016.03.005>
- 852 Brunet, J.; Fritz, Ö.; Richnau, G. (2010). *Biodiversity in European beech forests—A*  
853 *review with recommendations for sustainable forest management*. *Ecol. Bull.* 53,  
854 77–94, Available online: <http://www.jstor.org/stable/41442021>
- 855 Bonan, G. B., Lawrence, P. J., Oleson, K. W., Levis, S., Jung, M., Reichstein, M.,  
856 Lawrence, D. M., & Swenson, S. C. (2011). *Improving canopy processes in the*  
857 *Community Land Model version 4 (CLM4) using global flux fields empirically*  
858 *inferred from FLUXNET data*. *Journal of Geophysical Research Atmospheres*,  
859 116(G2). <https://doi.org/10.1029/2010jg001593>
- 860 Chmura, D. J., Banach, J., Kempf, M., Kowalczyk, J., Mohytych, V., Szeligowski, H.,  
861 Buraczyk, W., & Kowalkowski, W. (2024). *Growth and productivity of European*  
862 *beech populations show plastic response to climatic transfer at the north-eastern*  
863 *border of the species range*. *Forest Ecology and Management*, 565, 122043.  
864 <https://doi.org/10.1016/j.foreco.2024.122043>
- 865 Collalti, A., Perugini, L., Santini, M., Chiti, T., Nolè, A., Matteucci, G., Valentini, R. (2014).  
866 *A process-based model to simulate growth in forests with complex structure:*  
867 *Evaluation and use of 3D-CMCC Forest Ecosystem Model in a deciduous forest in*  
868 *Central Italy*. *Ecol. Modell.* 272, 362–378.  
869 <https://doi.org/10.1016/j.ecolmodel.2013.09.016>
- 870 Collalti, A., Marconi, S., Ibrom, A., Trotta, C., Anav, A., D'andrea, E., Matteucci, G.,  
871 Montagnani, L., Gielen, B., Mammarella, I., Grünwald, T., Knohl, A., Berninger, F.,  
872 Zhao, Y., Valentini, R., Santini, M. (2016). *Validation of 3D-CMCC Forest Ecosystem*

- 873 *Model (v.5.1) against eddy covariance data for 10 European forest sites*. *Geosci.*  
874 *Model Dev.* 9, 479–504. <https://doi.org/10.5194/gmd-9-479-2016>
- 875 Collalti, A., Biondo, C., Buttafuoco, G., Maesano, M., Caloiero, T., Lucà, F., Pellicone, G.,  
876 Ricca, N., Salvati, R., Veltri, A., Mugnozza, G. S., & Matteucci, G. (2017). *Simulation,*  
877 *calibration and validation protocols for the model 3D-CMCC-CNR-FEM: a case*  
878 *study in the Bonis' watershed (Calabria, Italy)*. *Forest@*, 14(4), 247–256.  
879 <https://doi.org/10.3832/efor2368-014>
- 880 Collalti, A., Trotta, C., Keenan, T.F., Ibrom, A., Bond-Lamberty, B., Grote, R., Vicca, S.,  
881 Reyer, C.P.O., Migliavacca, M., Veroustraete, F., Anav, A., Campioli, M.,  
882 Scoccimarro, E., Šigut, L., Grieco, E., Cescatti, A., Matteucci, G. (2018). *Thinning*  
883 *Can Reduce Losses in Carbon Use Efficiency and Carbon Stocks in Managed*  
884 *Forests Under Warmer Climate*. *J. Adv. Model. Earth Syst.* 10, 2427–2452.  
885 <https://doi.org/10.1029/2018MS001275>
- 886 Collalti, A., Thornton, P.E., Cescatti, A., Rita, A., Borghetti, M., Nolè, A., Trotta, C., Ciais,  
887 P., Matteucci, G. (2019). *The sensitivity of the forest carbon budget shifts across*  
888 *processes along with stand development and climate change*. *Ecol. Appl.* 29, 1–  
889 18. <https://doi.org/10.1002/eap.1837>
- 890 Collalti, A., Tjoelker, M.G., Hoch, G., Mäkelä, A., Guidolotti, G., Heskell, M., Petit, G., Ryan,  
891 M.G., Battipaglia, G., Matteucci, G., Prentice, I.C. (2020). *Plant respiration:*  
892 *Controlled by photosynthesis or biomass?* *Glob. Chang. Biol.* 26, 1739–1753.  
893 <https://doi.org/10.1111/gcb.14857>
- 894 Collalti, A., Dalmonech, D., Marano, G., Vangi, E., Puchi, P., Grieco, E., Orrico, M. (2023).  
895 *3D-CMCC-FEM (Coupled Model Carbon Cycle). BioGeoChemical and Biophysical*  
896 *Forest Ecosystem - User's Guide*. CNR Edizioni; ISBN 978-88-8080-573-1  
897 (electronic edition) <https://doi.org/10.32018/3D-CMCC-FEM-2022>;
- 898 Collalti, A. and Dalmonech, D. and Vangi, E. and Marano, G. and Puchi, P.F. and  
899 Morichetti, M. and Saponaro, V. and Orrico, M.R. and Grieco, E. (2024) *Monitoring*  
900 *and Predicting Forest Growth and Dynamics*. CNR Edizioni, Roma.
- 901 Collatz, G.J., Ball, J.T., Grivet, C. & Berry, J.A. (1991). *Physiological and environmental*  
902 *regulation of stomatal conductance, photosynthesis and transpiration: A model*  
903 *that includes a laminar boundary layer*. *Agricultural and Forest Meteorology*, 54,  
904 107–136.
- 905 Communication from the Commission to the European Parliament, the Council, the  
906 European Economic and Social Committee and the Committee of the Regions:  
907 *Forging a climate-resilient Europe - the new EU Strategy on Adaptation to*  
908 *Climate Change* - COM(2021) 82 final.
- 909 Dalmonech, D., Marano, G., Amthor, J.S., Cescatti, A., Lindner, M., Trotta, C., Collalti, A.  
910 (2022). *Feasibility of enhancing carbon sequestration and stock capacity in*  
911 *temperate and boreal European forests via changes to management regimes*.  
912 *Agric. For. Meteorol.* 327, 109203. <https://doi.org/10.1016/j.agrformet.2022.109203>
- 913 Dalmonech, D., Vangi, E., Chiesi, M., Chirici, G., Fibbi, L., Giannetti, F., Marano, G.,  
914 Massari, C., Nolè, A., Xiao, J., & Collalti, A. (2024). *Regional estimates of gross*  
915 *primary production applying the Process-Based Model 3D-CMCC-FEM vs.*  
916 *Remote-Sensing multiple datasets*. *European Journal of Remote Sensing*, 57(1).  
917 <https://doi.org/10.1080/22797254.2023.2301657>
- 918 De Cáceres, M., Mencuccini, M., Martin-StPaul, N., Limousin, J. M., Coll, L., Poyatos, R.,  
919 Cabon, A., Granda, V., Forner, A., Valladares, F., & Martínez-Vilalta, J. (2021).  
920 *Unravelling the effect of species mixing on water use and drought stress in*  
921 *Mediterranean forests: A modelling approach*. *Agricultural and Forest*  
922 *Meteorology*, 296, 108233. <https://doi.org/10.1016/j.agrformet.2020.108233>
- 923 De Cáceres, M., Molowny-Horas, R., Cabon, A., Martínez-Vilalta, J., Mencuccini, M.,  
924 García-Valdés, R., Nadal-Sala, D., Sabaté, S., Martin-StPaul, N., Morin, X.,

- 925 D'Adamo, F., Batllori, E., & Améztegui, A. (2023). *MEDFATE 2.9.3: a trait-enabled*  
926 *model to simulate Mediterranean forest function and dynamics at regional scales.*  
927 *Geoscientific Model Development*, 16(11), 3165–3201. [https://doi.org/10.5194/gmd-](https://doi.org/10.5194/gmd-16-3165-2023)  
928 [16-3165-2023](https://doi.org/10.5194/gmd-16-3165-2023)
- 929 De Cinti, B., Bombi, P., Ferretti, F., Cantiani, P., Di Salvatore, U., SimonÄ·iÄ·, P., Kutnar, L.,  
930 Åœater, M., GarfÄ·, V., Mason, F., & Matteucci, G. (2016). *From the experience of*  
931 *LIFE+ ManFor C.BD to the Manual of Best Practices in Sustainable Forest*  
932 *Management.* *Italian Journal of Agronomy*, 11(s1), 1–175.  
933 <https://doi.org/10.4081/ija.2016.789>
- 934 De Pury, D.G.G., Farquhar, G.D., 1997. *Simple scaling of photosynthesis from leaves to*  
935 *canopies without the errors of big-leaf models.* *Plant, Cell Environ.* 20, 537–557.  
936 <https://doi.org/10.1111/j.1365-3040.1997.00094.x>
- 937 De Wergifosse, L., Andr e, F., Goosse, H., Boczon, A., Cecchini, S., Ciceu, A., Collalti, A.,  
938 Cools, N., D'Andrea, E., De Vos, B., Hamdi, R., Ingerslev, M., Knudsen, M. A.,  
939 Kowalska, A., Leca, S., Matteucci, G., Nord-Larsen, T., Sanders, T. G., Schmitz, A.,  
940 Termonia, A., Vanguelova, E., Van Schaeybroeck, B., Verstraeten, A. Vesterdal, L.,  
941 Jonard, M. (2022). *Simulating tree growth response to climate change in*  
942 *structurally diverse oak and beech forests.* *The Science of the Total Environment*,  
943 806, 150422. <https://doi.org/10.1016/j.scitotenv.2021.150422>
- 944 Deb Burman, P. K., A. G. , P., Chakraborty, S., Tiwari, Y. K., Sarma, D., & Gogoi, N.  
945 (2024). *Simulating the ecosystem-atmosphere carbon, water and energy fluxes*  
946 *at a subtropical Indian forest using an ecosystem model.* *Ecological Modelling*,  
947 490, 110637. <https://doi.org/10.1016/j.ecolmodel.2024.110637>
- 948 Diaconu, D., Kahle, H. P., & Spiecker, H. (2017). *Thinning increases drought tolerance of*  
949 *European beech: a case study on two forested slopes on opposite sides of a*  
950 *valley.* *European Journal of Forest Research*, 136(2), 319–328.  
951 <https://doi.org/10.1007/s10342-017-1033-8>
- 952 Dufrene, E., Davi, H., Fran ois, C., Maire, G. L., Dantec, V. L., & Granier, A. (2005).  
953 *Modelling carbon and water cycles in a beech forest.* *Ecological Modelling*, 185(2–  
954 4), 407–436. <https://doi.org/10.1016/j.ecolmodel.2005.01.004>
- 955 Durrant, H. T., de Rigo, D., Caudullo, G. (2016). *Fagus sylvatica and other beeches in*  
956 *Europe: distribution, habitat, usage and threats.* In: San-Miguel-Ayanz, J., de Rigo,  
957 D., Caudullo, G., Houston Durrant, T., Mauri, A. (Eds.), *European Atlas of Forest*  
958 *Tree Species.* Publ. Off. EU, Luxembourg, pp. e012b90+
- 959 Farquhar, G.D., Caemmerer, S., Berry, J.A. (1980). *A biochemical model of*  
960 *photosynthetic CO<sub>2</sub> assimilation in leaves of C<sub>3</sub> species.* *Planta* 149, 78–90–90.
- 961 Fibbi, L., Moriondo, M., Chiesi, M., Bindi, M., & Maselli, F. (2019). *Impacts of climate*  
962 *change on the gross primary production of Italian forests.* *Annals of Forest*  
963 *Science*, 76(2). <https://doi.org/10.1007/s13595-019-0843-x>
- 964 Giuggiola, A., Zweifel, R., Feichtinger, L. M., Vollenweider, P., Bugmann, H., Haeni, M., &  
965 Rigling, A. (2018). *Competition for water in a xeric forest ecosystem – Effects of*  
966 *understory removal on soil micro-climate, growth and physiology of dominant*  
967 *Scots pine trees.* *Forest Ecology and Management*, 409, 241–249.  
968 <https://doi.org/10.1016/j.foreco.2017.11.002>
- 969 Grossiord, C., Buckley, T. N., Cernusak, L. A., Novick, K. A., Poulter, B., Siegwolf, R. T.  
970 W., Sperry, J. S., & McDowell, N. G. (2020). *Plant responses to rising vapor*  
971 *pressure deficit.* *New Phytologist*, 226(6), 1550–1566.  
972 <https://doi.org/10.1111/nph.16485>
- 973 Guillemot, J., Delpierre, N., Vallet, P., Fran ois, C., Martin-StPaul, N. K., Soudani, K.,  
974 Nicolas, M., Badeau, V., & Dufr ene, E. (2014). *Assessing the effects of management*  
975 *on forest growth across France: insights from a new functional–structural model.*  
976 *Annals of Botany*, 114(4), 779–793. <https://doi.org/10.1093/aob/mcu059>

- 977 Hölttä, T., Cochard, H., Nikinmaa, E., & Mencuccini, M. (2009). *Capacitive effect of*  
978 *cavitation in xylem conduits: results from a dynamic model*. *Plant, Cell &*  
979 *Environment/Plant, Cell and Environment*, 32(1), 10–21.  
980 <https://doi.org/10.1111/j.1365-3040.2008.01894.x>
- 981 Jarvis, P. G. (1976). *The Interpretation of the Variations in Leaf Water Potential and*  
982 *Stomatal Conductance Found in Canopies in the Field*. *Philosophical Transactions*  
983 *of the Royal Society B: Biological Sciences*, 273(927), 593–610.  
984 doi:10.1098/rstb.1976.0035
- 985 Jarvis, N.J., Jansson, P-E., Dik, P.E., Messing, I. (1991). *Modelling water and solute*  
986 *transport in macroporous soil*. I. Model description and sensitivity analysis. *Journal*  
987 *of Soil Science*, 42, 59–70.
- 988 Kane, C., & McAdam, S. (2023). *Abscisic acid driven stomatal closure during drought*  
989 *in anisohydric Fagus sylvatica*. *Journal of Plant Hydraulics*, 9, 002.  
990 <https://doi.org/10.20870/jph.2023.002>
- 991 Kattge, J., Knorr, W., (2007). Temperature acclimation in a biochemical model of  
992 photosynthesis: A reanalysis of data from 36 species. *Plant, Cell Environ.* 30, 1176–  
993 1190. <https://doi.org/10.1111/j.1365-3040.2007.01690.x>
- 994 Kimmins, (Hamish) J. P., Blanco, J. A., Seely, B., Welham, C., & Scoullar, K. (2008).  
995 *Complexity in modelling forest ecosystems: How much is enough?* *Forest Ecology*  
996 *and Management*, 256(10), 1646–1658. <https://doi.org/10.1016/j.foreco.2008.03.011>
- 997 Kramer, K., Leinonen, I., Bartelink, H., Berbigier, P., Borghetti, M., Bernhofer, C.,  
998 Cienciala, E., Dolman, A., Froer, O., Gracia, A., Granier, A., Grünwald, T., Hari, P.,  
999 Jans, W., Kellomäki, S., Loustau, D., Magnani, F., Markkanen, T., Matteucci, G.,  
1000 Mohren, G.M.J., Moors, E., Nissinen, A., Peltola, H. Sabaté, S., Sanchez, A. (2002).  
1001 *Evaluation of six process-based forest growth models using eddy-covariance*  
1002 *measurements of CO2 and H2O fluxes at six forest sites in Europe*. *Global Change*  
1003 *Biology*, 8(3), 213–230. <https://doi.org/10.1046/j.1365-2486.2002.00471.x>
- 1004 Larsbo, M., Roulier, S., Stenemo, F., Kasteel, R., Jarvis, N. (2005). *An Improved*  
1005 *Dual-Permeability Model of Water Flow and Solute Transport in the Vadose Zone*.  
1006 *Vadose Zone Journal*, 4, 398–406.
- 1007 Leuning, R. (2002). *Temperature dependence of two parameters in a photosynthesis*  
1008 *model*. *Plant, Cell and Environment*, 25, 1205–1210.
- 1009 Leuschner, C., Schipka, F., & Backes, K. (2021). *Stomatal regulation and water potential*  
1010 *variation in European beech: challenging the iso/anisohydry concept*. *Tree*  
1011 *Physiology*, 42(2), 365–378. <https://doi.org/10.1093/treephys/tpab104>
- 1012 Loescher, H. W., Law, B. E., Mahrt, L., Hollinger, D. Y., Campbell, J., & Wofsy, S. C.  
1013 (2006). *Uncertainties in, and interpretation of, carbon flux estimates using the*  
1014 *eddy covariance technique*. *Journal of Geophysical Research Atmospheres*,  
1015 111(D21). <https://doi.org/10.1029/2005jd006932>
- 1016 Lombardi, D., Micalizzi, K., & Vitale, M. (2023). *Assessing carbon and water fluxes in a*  
1017 *mixed Mediterranean protected forest under climate change: An integrated*  
1018 *bottom – up and top – down approach*. *Ecological Informatics*, 78, 102318.  
1019 <https://doi.org/10.1016/j.ecoinf.2023.102318>
- 1020 Lüttschwager, D., & Jochheim, H. (2020). *Drought Primarily Reduces Canopy*  
1021 *Transpiration of Exposed Beech Trees and Decreases the Share of Water Uptake*  
1022 *from Deeper Soil Layers*. *Forests*, 11(5), 537. <https://doi.org/10.3390/f11050537>
- 1023 Huber, M. O., Eastaugh, C. S., Gschwantner, T., Hasenauer, H., Kindermann, G.,  
1024 Ledermann, T., Lexer, M. J., Rammer, W., Schörghuber, S., & Sterba, H. (2013).  
1025 *Comparing simulations of three conceptually different forest models with*  
1026 *National Forest Inventory data*. *Environmental Modelling & Software*, 40, 88–97.  
1027 <https://doi.org/10.1016/j.envsoft.2012.08.003>



- 1028 INFC (2015). Inventario Nazionale delle Foreste e dei Serbatoi Forestali di Carbonio.  
1029 Ministero delle Politiche Agricole Alimentari e Forestali, Ispettorato Generale –  
1030 Corpo Forestale dello Stato, CRA – Istituto Sperimentale per l’Assestamento  
1031 Forestale e per l’Alpicoltura. [online] URL:  
1032 [https://www.inventarioforestale.org/it/statistiche\\_inf/](https://www.inventarioforestale.org/it/statistiche_inf/)  
1033 Italiano, S. S., Camarero, J. J., Borghetti, M., Colangelo, M., Rita, A., & Ripullone, F.  
1034 (2024). *Drought legacies in mixed Mediterranean forests: Analysing the effects of*  
1035 *structural overshoot, functional traits and site factors*. *The Science of the Total*  
1036 *Environment*, 927, 172166. <https://doi.org/10.1016/j.scitotenv.2024.172166>  
1037 Mahnken, M., Cailleret, M., Collalti, A., Trotta, C., Biondo, C., D’Andrea, E., Dalmonech,  
1038 D., Marano, G., Mäkelä, A., Minunno, F., Peltoniemi, M., Trotsiuk, V., Nadal-Sala, D.,  
1039 Sabaté, S., Vallet, P., Aussenac, R., Cameron, D. R., Bohn, F. J., Grote, R.,  
1040 Augustynczyk, A. L. D., Yousefpour, R., Huber, N., Bugmann, H., Merganičová, K.,  
1041 Merganic, J., Valent, P., Lasch-Born, P., Hartig, F., Vega del Valle, I. D., Volkholz, J.,  
1042 Gutsch, M., Matteucci, G., Krejza, J., Ibrom, A., Meesenburg, H., Rötzer, T., van der  
1043 Maaten-Theunissen, M., van der Maaten, E., & Reyer, C. P. O. (2022). *Accuracy,*  
1044 *realism and general applicability of European forest models*. *Global Change*  
1045 *Biology*, 28(23), 6921–6943. <https://doi.org/10.1111/gcb.16384>  
1046 Maréchaux, I., Langerwisch, F., Huth, A., Bugmann, H., Morin, X., Reyer, C. P., Seidl, R.,  
1047 Collalti, A., De Paula, M. D., Fischer, R., Gutsch, M., Lexer, M. J., Lischke, H.,  
1048 Rammig, A., Rödig, E., Sakschewski, B., Taubert, F., Thonicke, K., Vacchiano, G., &  
1049 Bohn, F. J. (2021). *Tackling unresolved questions in forest ecology: The past and*  
1050 *future role of simulation models*. *Ecology and Evolution*, 11(9), 3746–3770.  
1051 <https://doi.org/10.1002/ece3.7391>  
1052 Martínez-Vilalta, J., Sala, A., Asensio, D., Galiano, L., Hoch, G., Palacio, S., Piper, F. I., &  
1053 Lloret, F. (2016). *Dynamics of non-structural carbohydrates in terrestrial plants: a*  
1054 *global synthesis*. *Ecological Monographs*, 86(4), 495–516.  
1055 <https://doi.org/10.1002/ecm.1231>  
1056 Medlyn, B. E., Badeck, F. W., De Pury, D. G. G., Barton, C. V. M., Broadmeadow, M.,  
1057 Ceulemans, R., De Angelis, P., Forstreuter, M., Jach, M. E., Kellomäki, S., Laitat, E.,  
1058 Marek, M., Philippot, S., Rey, A., Strassmeyer, J., Laitinen, K., Liozon, R., Portier, B.,  
1059 Roberntz, P., Wang, K., Jarvis, P. G. (1999). *Effects of elevated [CO<sub>2</sub>] on*  
1060 *photosynthesis in European forest species: a meta-analysis of model parameters*.  
1061 *Plant Cell & Environment*, 22(12), 1475–1495. [https://doi.org/10.1046/j.1365-](https://doi.org/10.1046/j.1365-3040.1999.00523.x)  
1062 [3040.1999.00523.x](https://doi.org/10.1046/j.1365-3040.1999.00523.x)  
1063 Merganičová, K., Merganič, J., Lehtonen, A., Vacchiano, G., Sever, M. Z. O.,  
1064 Augustynczyk, A. L. D., Grote, R., Kyselová, I., Mäkelä, A., Yousefpour, R., Krejza, J.,  
1065 Collalti, A., & Reyer, C. P. O. (2019). *Forest carbon allocation modelling under*  
1066 *climate change*. *Tree Physiology*, 39(12), 1937–1960.  
1067 <https://doi.org/10.1093/treephys/tpz105>  
1068 Monteith, J. L. and M. H. Unsworth (2008). *Principles of Environmental Physics, 3rd*  
1069 *Edition*. Burlington, MA, Academic Press <https://doi.org/10.3832/ifer1802-009>  
1070 Morichetti, M., Vangi, E., & Collalti, A. (2024). *Predicted Future Changes in the Mean*  
1071 *Seasonal Carbon Cycle Due to Climate Change*. *Forests*, 15(7), 1124.  
1072 <https://doi.org/10.3390/f15071124>  
1073 Noce, S., Collalti, A., & Santini, M. (2017). *Likelihood of changes in forest species*  
1074 *suitability, distribution, and diversity under future climate: The case of Southern*  
1075 *Europe*. *Ecology and Evolution*, 7(22), 9358–9375.  
1076 <https://doi.org/10.1002/ece3.3427>

- 1077 Noce, S., Cipriano, C., & Santini, M. (2023). *Altitudinal shifting of major forest tree*  
1078 *species in Italian mountains under climate change*. *Frontiers in Forests and Global*  
1079 *Change*, 6. <https://doi.org/10.3389/ffgc.2023.1250651>
- 1080 Papale, D., Reichstein, M., Aubinet, M., Canfora, E., Bernhofer, C., Kutsch, W. L.,  
1081 Longdoz, B., Rambal, S., Valentini, R., Vesala, T., & Yakir, D. (2006). *Towards a*  
1082 *standardized processing of Net Ecosystem Exchange measured with eddy*  
1083 *covariance technique: algorithms and uncertainty estimation*. *Biogeosciences*,  
1084 3(4), 571–583. <https://doi.org/10.5194/bg-3-571-2006>
- 1085 Pastorello, G., Trotta, C., Canfora, E., Chu, H., Christianson, D., Cheah, Y.W., Poindexter,  
1086 C., Chen, J., Elbashandy, A., Humphrey, M., Isaac, P., Polidori, D., Reichstein, M.,  
1087 Ribeca, A., van Ingen, C., Vuichard, N., Zhang, L., Amiro, B., Ammann, C., Arain,  
1088 M.A., Ardö, J., Arkebauer, T., Arndt, S.K., Arriga, N., Aubinet, M., Aurela, M.,  
1089 Baldocchi, D., Barr, A., Beamesderfer, E., Beletti Marchesini, L., Bergeron, O.,  
1090 Beringer, J., Bernhofer, C., Berveiller, D., Billesbach, D., Black, T.A., Blanken, P.D.,  
1091 Bohrer, G., Boike, J., Bolstad, P.V., Bonal, D., Bonnefond, J.-M., Bowling, D.R.,  
1092 Bracho, R., Brodeur, J., Brümmer, C., Buchmann, N., Burban, B., Burns, S.P., Buysse,  
1093 P., Cale, P., Cavagna, M., Cellier, P., Chen, S., Chini, I., Christensen, T.R., Cleverly, J.,  
1094 Collalti, A., Consalvo, C., Cook, B.D., Cook, D., Coursolle, C., Cremonese, E., Curtis,  
1095 P.S., D'Andrea, E., da Rocha, H., Dai, X., Davis, K.J., De Cinti, B., de Grandcourt, A.,  
1096 De Ligne, A., De Oliveira, R.C., Delpierre, N., Desai, A.R., Di Bella, C.M., di Tommasi,  
1097 P., Dolman, H., Domingo, F., Dong, G., Dore, S., Duce, P., Dufrêne, E., Dunn, A.,  
1098 Dušek, J., Eamus, D., Eichelmann, U., ElKhidir, H.A.M., Eugster, W., Ewenz, C.M.,  
1099 Ewers, B., Famulari, D., Fares, S., Feigenwinter, I., Feitz, A., Fensholt, R., Filippa, G.,  
1100 Fischer, M., Frank, J., Galvagno, M., Gharun, M., Gianelle, D., Gielen, B., Gioli, B.,  
1101 Gitelson, A., Goded, I., Goeckede, M., Goldstein, A.H., Gough, C.M., Goulden, M.L.,  
1102 Graf, A., Griebel, A., Gruening, C., Grünwald, T., Hammerle, A., Han, S., Han, X.,  
1103 Hansen, B.U., Hanson, C., Hatakka, J., He, Y., Hehn, M., Heinesch, B., Hinko-Najera,  
1104 N., Hörtnagl, L., Hutley, L., Ibrom, A., Ikawa, H., Jackowicz-Korczynski, M., Janouš,  
1105 D., Jans, W., Jassal, R., Jiang, S., Kato, T., Khomik, M., Klatt, J., Knohl, A., Knox, S.,  
1106 Kobayashi, H., Koerber, G., Kolle, O., Kosugi, Y., Kotani, A., Kowalski, A., Kruijt, B.,  
1107 Kurbatova, J., Kutsch, W.L., Kwon, H., Launiainen, S., Laurila, T., Law, B., Leuning,  
1108 R., Li, Y., Liddell, M., Limousin, J.-M., Lion, M., Liska, A.J., Lohila, A., López-  
1109 Ballesteros, A., López-Blanco, E., Loubet, B., Loustau, D., Lucas-Moffat, A., Lüers, J.,  
1110 Ma, S., Macfarlane, C., Magliulo, V., Maier, R., Mammarella, I., Manca, G., Marcolla,  
1111 B., Margolis, H.A., Marras, S., Massman, W., Mastepanov, M., Matamala, R.,  
1112 Matthes, J.H., Mazzenga, F., McCaughey, H., McHugh, I., McMillan, A.M.S., Merbold,  
1113 L., Meyer, W., Meyers, T., Miller, S.D., Minerbi, S., Moderow, U., Monson, R.K.,  
1114 Montagnani, L., Moore, C.E., Moors, E., Moreaux, V., Moureaux, C., Munger, J.W.,  
1115 Nakai, T., Neiryneck, J., Nesic, Z., Nicolini, G., Noormets, A., Northwood, M., Noretto,  
1116 M., Nouvellon, Y., Novick, K., Oechel, W., Olesen, J.E., Ourcival, J.-M., Papuga, S.A.,  
1117 Parmentier, F.-J., Paul-Limoges, E., Pavelka, M., Peichl, M., Pendall, E., Phillips, R.P.,  
1118 Pilegaard, K., Pirk, N., Posse, G., Powell, T., Prasse, H., Prober, S.M., Rambal, S.,  
1119 Rannik, Ü., Raz-Yaseef, N., Rebmann, C., Reed, D., Resco de Dios, V., Restrepo-  
1120 Coupe, N., Reverter, B.R., Roland, M., Sabbatini, S., Sachs, T., Saleska, S.R.,  
1121 Sánchez-Cañete, E.P., Sanchez-Mejia, Z.M., Schmid, H.P., Schmidt, M., Schneider,  
1122 K., Schrader, F., Schroder, I., Scott, R.L., Sedláč, P., Serrano-Ortiz, P., Shao, C., Shi,  
1123 P., Shironya, I., Siebicke, L., Šigut, L., Silberstein, R., Sirca, C., Spano, D.,  
1124 Steinbrecher, R., Stevens, R.M., Sturtevant, C., Suyker, A., Tagesson, T., Takanashi,  
1125 S., Tang, Y., Tapper, N., Thom, J., Tomassucci, M., Tuovinen, J.-P., Urbanski, S.,  
1126 Valentini, R., van der Molen, M., van Gorsel, E., van Huissteden, K., Varlagin, A.,  
1127 Verfaillie, J., Vesala, T., Vincke, C., Vitale, D., Vygodskaya, N., Walker, J.P., Walter-  
1128 Shea, E., Wang, H., Weber, R., Westermann, S., Wille, C., Wofsy, S., Wohlfahrt, G.,

- 1129 Wolf, S., Woodgate, W., Li, Y., Zampedri, R., Zhang, J., Zhou, G., Zona, D., Agarwal,  
1130 D., Biraud, S., Torn, M., & Papale, D. (2020). *The FLUXNET2015 dataset and the*  
1131 *ONEFlux processing pipeline for eddy covariance data*. *Scientific Data*, 7(1).  
1132 <https://doi.org/10.1038/s41597-020-0534-3>
- 1133 Pan, Y., Birdsey, R. A., Phillips, O. L., Houghton, R. A., Fang, J., Kauppi, P. E., Keith, H.,  
1134 Kurz, W. A., Ito, A., Lewis, S. L., Nabuurs, G. J., Shvidenko, A., Hashimoto, S., Lerink,  
1135 B., Schepaschenko, D., Castanho, A., & Murdiyarsa, D. (2024). *The enduring world*  
1136 *forest carbon sink*. *Nature*, 631(8021), 563–569. [https://doi.org/10.1038/s41586-](https://doi.org/10.1038/s41586-024-07602-x)  
1137 [024-07602-x](https://doi.org/10.1038/s41586-024-07602-x)
- 1138 Petrik, P., Petek-Petrik, A., Kurjak, D., Mukarram, M., Klein, T., Gömöry, D., Střelcová, K.,  
1139 Frýdl, J., & Konôpková, A. (2022). *Interannual adjustments in stomatal and leaf*  
1140 *morphological traits of European beech (Fagus sylvatica L.) demonstrate its*  
1141 *climate change acclimation potential*. *Plant Biology*, 24(7), 1287–1296.  
1142 <https://doi.org/10.1111/plb.13401>
- 1143 Pietsch, S. A., Hasenauer, H., & Thornton, P. E. (2005). *BGC-model parameters for tree*  
1144 *species growing in central European forests*. *Forest Ecology and Management*,  
1145 211(3), 264–295. <https://doi.org/10.1016/j.foreco.2005.02.046>
- 1146 Pilli, R., Alkama, R., Cescatti, A., Kurz, W. A., & Grassi, G. (2022). *The European forest*  
1147 *carbon budget under future climate conditions and current management*  
1148 *practices*. *Biogeosciences*, 19(13), 3263–3284. [https://doi.org/10.5194/bg-19-3263-](https://doi.org/10.5194/bg-19-3263-2022)  
1149 [2022](https://doi.org/10.5194/bg-19-3263-2022)
- 1150 Piovesan, G., Biondi, F., Di Filippo, A., Alessandrini, A., & Maugeri, M. (2008).  
1151 *Drought-driven growth reduction in old beech (Fagus sylvatica L.) forests of the*  
1152 *central Apennines, Italy*. *Global Change Biology*, 14(6), 1265–1281.  
1153 <https://doi.org/10.1111/j.1365-2486.2008.01570.x>
- 1154 Priwitzer, T., Kurjak, D., Kmeť, J., Sitková, Z., & Leštianska, A. (2014). *Photosynthetic*  
1155 *response of European beech to atmospheric and soil drought*. *Central European*  
1156 *Forestry Journal*, 60(1), 32–38. <https://doi.org/10.2478/forj-2014-0003>
- 1157 Puchi, P. F., Dalmonech, D., Vangi, E., Battipaglia, G., Tognetti, R., & Collalti, A. (2024).  
1158 *Contrasting patterns of water use efficiency and annual radial growth among*  
1159 *European beech forests along the Italian peninsula*. *Scientific Reports*, 14(1).  
1160 <https://doi.org/10.1038/s41598-024-57293-7>
- 1161 Pukkala, T. (2016). *Which type of forest management provides most ecosystem*  
1162 *services?* *Forest Ecosystems/Forest Ecosystems*, 3(1).  
1163 <https://doi.org/10.1186/s40663-016-0068-5>
- 1164 Raffa, M., Adinolfi, M., Reder, A. et al. (2023). *Very High Resolution Projections over*  
1165 *Italy under different CMIP5 IPCC scenarios*. *Sci Data* 10, 238 .  
1166 <https://doi.org/10.1038/s41597-023-02144-9>
- 1167 Reyer, C., Lasch-Born, P., Suckow, F., Gutsch, M., Murawski, A., & Pilz, T. (2013).  
1168 *Projections of regional changes in forest net primary productivity for different tree*  
1169 *species in Europe driven by climate change and carbon dioxide*. *Annals of Forest*  
1170 *Science*, 71(2), 211–225. <https://doi.org/10.1007/s13595-013-0306-8>
- 1171 Reyer, C., Silveyra Gonzalez, R., Dolos, K., Hartig, F., Hauf, Y., Noack, M., Lasch-Born, P.,  
1172 Rötzer, T., Pretzsch, H., Meesenburg, H., Fleck, S., Wagner, M., Bolte, A., Sanders,  
1173 T., Kolari, P., Mäkelä, A., Vesala, T., Mammarella, I., Pumpanen, J., Matteucci, G.,  
1174 Collalti, A., D'Andrea, E., Foltýnová, L., Krejza, J., Ibrom, A., Pilegaard, K., Loustau,  
1175 D., Bonnefond, J.-M., Berbigier, P., Picart, D., Lafont, S., Dietze, M., Cameron, D.,  
1176 Vieno, M., Tian, H., Palacios-Orueta, A., Cicuendez, V., Recuero, L., Wiese, K.,  
1177 Büchner, M., Lange, S., Volkholz, J., Kim, H., Weedon, G., Sheffield, J., Vega del  
1178 Valle, I., Suckow, F., Horemans, J., Martel, S., Bohn, F., Steinkamp, J., Chikalanov, A.,  
1179 Mahnken, M., Gutsch, M., Trotta, C., Babst, F., & Frieler, K. (2020a). *The*  
1180 *PROFOUND database for evaluating vegetation models and simulating climate*

- 1181 *impacts on European forests version V. 0.3.* GFZ Data Services.  
1182 <https://doi.org/10.5880/PIK.2020.006>
- 1183 Reyer, C. P. O., Silveyra Gonzalez, R., Dolos, K., Hartig, F., Hauf, Y., Noack, M., Lasch-  
1184 Born, P., Rötzer, T., Pretzsch, H., Meesenburg, H., Fleck, S., Wagner, M., Bolte, A.,  
1185 Sanders, T. G. M., Kolari, P., Mäkelä, A., Vesala, T., Mammarella, I., Pumpanen, J.,  
1186 Collalti, A., Trotta, C., Matteucci, G., D'Andrea, E., Foltýnová, L., Krejza, J., Ibrom, A.,  
1187 Pilegaard, K., Loustau, D., Bonnefond, J.-M., Berbigier, P., Picart, D., Lafont, S.,  
1188 Dietze, M., Cameron, D., Vieno, M., Tian, H., Palacios-Orueta, A., Cicuendez, V.,  
1189 Recuero, L., Wiese, K., Büchner, M., Lange, S., Volkholz, J., Kim, H., Horemans, J. A.,  
1190 Bohn, F., Steinkamp, J., Chikalanov, A., Weedon, G. P., Sheffield, J., Babst, F., Vega  
1191 del Valle, I., Suckow, F., Martel, S., Mahnken, M., Gutsch, M., & Frieler, K. (2020b).  
1192 *The PROFOUND database for evaluating vegetation models and simulating*  
1193 *climate impacts on European forests.* Earth System Science Data, 12(2), 1295–1320.  
1194 <https://doi.org/10.5194/essd-12-1295-2020>
- 1195 Rezaie, N., D'Andrea, E., Bräuning, A., Matteucci, G., Bombi, P., & Lauteri, M. (2018). *Do*  
1196 *atmospheric CO2 concentration increase, climate and forest management affect*  
1197 *iWUE of common beech? Evidences from carbon isotope analyses in tree rings.*  
1198 *Tree Physiology*, 38(8), 1110–1126. <https://doi.org/10.1093/treephys/tpy025>
- 1199 Richardson, A.D., Black, T.A., Ciais, P., Delbart, N., Friedl, M.A., Gobron, N., Hollinger,  
1200 D.Y., Kutsch, W.L., Longdoz, B., Luysaert, S., Migliavacca, M., Montagnani, L.,  
1201 Munger, J.W., Moors, E., Piao, S., Rebmann, C., Reichstein, M., Saigusa, N.,  
1202 Tomelleri, E., Vargas, R., & Varlagin, A. (2010). *Influence of spring and autumn*  
1203 *phenological transitions on forest ecosystem productivity.* Philosophical  
1204 *Transactions - Royal Society. Biological Sciences*, 365(1555), 3227–3246.  
1205 <https://doi.org/10.1098/rstb.2010.0102>
- 1206 Rita, A., Bonanomi, G., Allevato, E., Borghetti, M., Cesarano, G., Mogavero, V., Rossi, S.,  
1207 Saulino, L., Zotti, M., & Saracino, A. (2021). *Topography modulates near-ground*  
1208 *microclimate in the Mediterranean Fagus sylvatica treeline.* Scientific Reports,  
1209 11(1). <https://doi.org/10.1038/s41598-021-87661-6>
- 1210 Riviere, M., Caurla, S., & Delacote, P. (2020). *Evolving Integrated Models From*  
1211 *Narrower Economic Tools: the Example of Forest Sector Models.* Environmental  
1212 *Modeling & Assessment*, 25(4), 453–469. [https://doi.org/10.1007/s10666-020-](https://doi.org/10.1007/s10666-020-09706-w)  
1213 [09706-w](https://doi.org/10.1007/s10666-020-09706-w)
- 1214 Rötzer, T., Dieler, J., Mette, T., Moshammer, R., & Pretzsch, H. (2010). *Productivity and*  
1215 *carbon dynamics in managed Central European forests depending on site*  
1216 *conditions and thinning regimes.* *Forestry: An International Journal of Forest*  
1217 *Research*, 83(5), 483–496. <https://doi.org/10.1093/forestry/cpq031>
- 1218 Ruffault, J., Pimont, F., Cochard, H., Dupuy, J.-L. & Martin-StPaul, N. (2022). *SurEau-*  
1219 *Ecos v2.0: A trait-based plant hydraulics model for simulations of plant water*  
1220 *status and drought-induced mortality at the ecosystem level.* Geoscientific Model  
1221 *Development*, 15, 5593–5626.
- 1222 Skrk, N., Martinez del Castillo, E., Serrano-Notivoli, R., Luis, M. De, Novak, K., Merela,  
1223 M., Cufar, K. (2023). *Spatial and temporal variation of Fagus sylvatica growth in*  
1224 *marginal areas under progressive climate change.* *Dendrochronologia* 81.  
1225 <https://doi.org/10.1016/j.dendro.2023.126135>
- 1226 Schmied, G., Pretzsch, H., Ambs, D., Uhl, E., Schmucker, J., Fäth, J., Biber, P., Hoffmann,  
1227 Y. D., Šeho, M., Mellert, K. H., & Hilmers, T. (2023). *Rapid beech decline under*  
1228 *recurrent drought stress: Individual neighborhood structure and soil properties*  
1229 *matter.* *Forest Ecology and Management*, 545, 121305.  
1230 <https://doi.org/10.1016/j.foreco.2023.121305>
- 1231 Simonin, K., Kolb, T., Montes-Helu, M., & Koch, G. (2007). *The influence of thinning on*  
1232 *components of stand water balance in a ponderosa pine forest stand during and*

- 1233 *after extreme drought*. *Agricultural and Forest Meteorology*, 143(3–4), 266–276.  
1234 <https://doi.org/10.1016/j.agrformet.2007.01.003>
- 1235 Sperry, J. S., Adler, F. R., Campbell, G. S., & Comstock, J. P. (1998). *Limitation of plant*  
1236 *water use by rhizosphere and xylem conductance: results from a model*. *Plant,*  
1237 *Cell & Environment/Plant, Cell and Environment*, 21(4), 347–359.  
1238 <https://doi.org/10.1046/j.1365-3040.1998.00287.x>
- 1239 Sperry, J.S., Venturas, M.D., Anderegg, W.R.L., Mencuccini, M., Mackay, D.S., Wang, Y.,  
1240 et al. (2017). *Predicting stomatal responses to the environment from the*  
1241 *optimization of photosynthetic gain and hydraulic cost*. *Plant, Cell & Environment*,  
1242 40, 816–830. <https://doi.org/10.1111/pce.12852>.
- 1243 Taylor, A. R., Chen, H. Y. H., & VanDamme, L. (2009). *A Review of Forest Succession*  
1244 *Models and Their Suitability for Forest Management Planning*. *Forest Science*,  
1245 55(1), 23–36. <https://doi.org/10.1093/forestscience/55.1.23>
- 1246 Tegel, W., Seim, A., Hakelberg, D., Hoffmann, S., Panev, M., Westphal, T., Büntgen, U.  
1247 (2014). *A recent growth increase of European beech (Fagus sylvatica L.) at its*  
1248 *Mediterranean distribution limit contradicts drought stress*. *Eur. J. For. Res.* 133,  
1249 61–71. <https://doi.org/10.1007/s10342-013-0737-7>
- 1250 Testolin, R., Dalmonch, D., Marano, G., Bagnara, M., D'Andrea, E., Matteucci, G., Noce,  
1251 S., Collalti, A. (2023). *Simulating diverse forest management options in a*  
1252 *changing climate on a Pinus nigra subsp. laricio plantation in Southern Italy*. *Sci.*  
1253 *Total Environ.* 857, 159361. <https://doi.org/10.1016/j.scitotenv.2022.159361>
- 1254 Thom, D., Buras, A., Heym, M., Klemmt, H. J., & Wauer, A. (2023). *Varying growth*  
1255 *response of Central European tree species to the extraordinary drought period of*  
1256 *2018 – 2020*. *Agricultural and Forest Meteorology*, 338, 109506.  
1257 <https://doi.org/10.1016/j.agrformet.2023.109506>
- 1258 Tognetti, R., Lasserre, B., Di Febbraro, M., & Marchetti, M. (2019). *Modeling regional*  
1259 *drought-stress indices for beech forests in Mediterranean mountains based on*  
1260 *tree-ring data*. *Agricultural and Forest Meteorology*, 265, 110–120.  
1261 <https://doi.org/10.1016/j.agrformet.2018.11.015>
- 1262 Vacchiano, G., Magnani, F., & Collalti, A. (2012). *Modeling Italian forests: state of the art*  
1263 *and future challenges*. *IForest*, 5(1), 113–120. <https://doi.org/10.3832/ifor0614-005>
- 1264 Vangi, E., Dalmonch, D., Cioccolo, E., Marano, G., Bianchini, L., Puchi, P. F., Grieco, E.,  
1265 Cescatti, A., Colantoni, A., Chirici, G., & Collalti, A. (2024a). *Stand age diversity and*  
1266 *climate change affects forests' resilience and stability, although unevenly*. bioRxiv  
1267 (Cold Spring Harbor Laboratory). <https://doi.org/10.1101/2023.07.12.548709>
- 1268 Vangi, E., Dalmonch, D., Cioccolo, E., Marano, G., Bianchini, L., Puchi, P. F., Grieco, E.,  
1269 Cescatti, A., Colantoni, A., Chirici, G., & Collalti, A. (2024b). *Stand age diversity*  
1270 *(and more than climate change) affects forests' resilience and stability, although*  
1271 *unevenly*. *Journal of Environmental Management*, 366, 121822.  
1272 <https://doi.org/10.1016/j.jenvman.2024.121822>
- 1273 Verbeeck, H., Samson, R., Granier, A. A., Montpied, P., & Lemeur, R. (2008). *Multi-year*  
1274 *model analysis of GPP in a temperate beech forest in France*. *Ecological*  
1275 *Modelling*, 210(1–2), 85–103. <https://doi.org/10.1016/j.ecolmodel.2007.07.010>
- 1276 Waring, R. H. and S. W. Running (2007). *Forest Ecosystems: Analysis at Multiple*  
1277 *Scales*. San Francisco, CA, Elsevier Academic Press.
- 1278 Yu, X., Orth, R., Reichstein, M., Bahn, M., Klosterhalfen, A., Knohl, A., Koepsch, F.,  
1279 Migliavacca, M., Mund, M., Nelson, J. A., Stocker, B. D., Walther, S., & Bastos, A.  
1280 (2022b). *Contrasting drought legacy effects on gross primary productivity in a*  
1281 *mixed versus pure beech forest*. *Biogeosciences*, 19(17), 4315–4329.  
1282 <https://doi.org/10.5194/bg-19-4315-2022>
- 1283 Zuccarini, P., Delpierre, N., Mariën, B., Peñuelas, J., Heinecke, T., Campioli, M. (2023).  
1284 *Drivers and dynamics of foliar senescence in temperate deciduous forest trees at*

1285 *their southern limit of distribution in Europe.* Agric. For. Meteorol. 342, 109716.  
1286 <https://doi.org/10.1016/j.agrformet.2023.109716>